Neuron

Cannabidiol modulates excitatory-inhibitory ratio to counter hippocampal hyperactivity

Graphical abstract

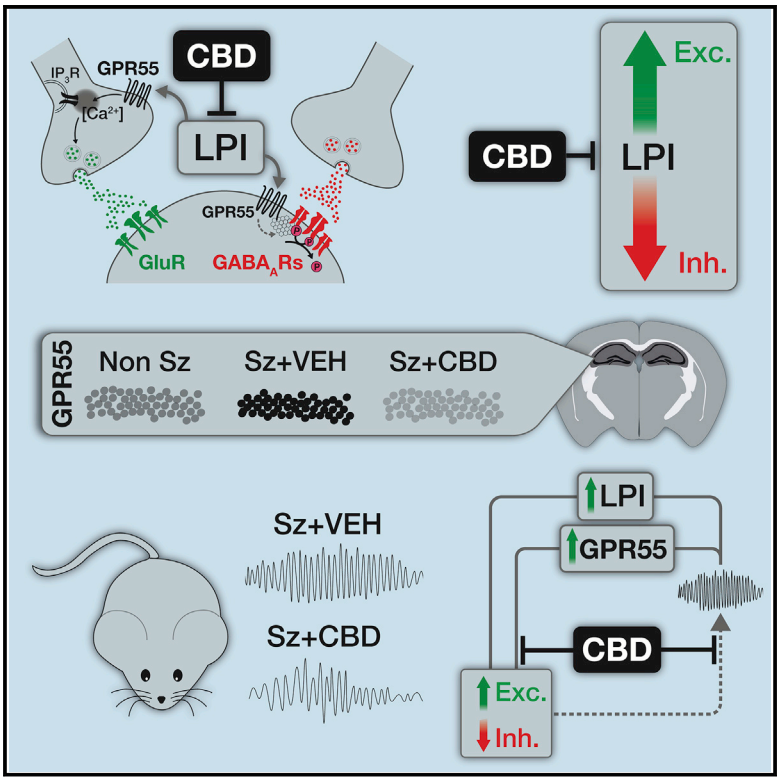

Highlights

- LPI, a GPR55 ligand, regulates the hippocampal E:I ratio
- LPI weakens postsynaptic inhibition through dispersal of γ_2 and gephyrin clusters
- Acute seizures upregulate GPR55 and LPI, producing a pernicious positive feedback loop
- CBD dampens elevation of E-I ratio and excitability, thus opposing recurrent seizures

Authors

Evan C. Rosenberg,
Simon Chamberland,
Michael Bazelot, ...,
Helen E. Scharfman,
Benjamin J. Whalley, Richard W. Tsien

Correspondence

richard.tsien@nyulangone.org

In brief

Rosenberg et al. reveal a potential mechanism by which cannabidiol (CBD) reduces seizures. They discover that CBD restores the hippocampal excitatory-to-inhibitory ratio by preventing the actions of the lipid LPI at the receptor GPR55. Seizures acutely potentiate the GPR55-LPI axis, providing a target for CBD's anti-seizure action.

Rosenberg et al., 2023, Neuron *111*, 1–19
April 19, 2023
https://doi.org/10.1016/j.neuron.2023.01.018

CellPress

Please cite this article in press as: Rosenberg et al., Cannabidiol modulates excitatory-inhibitory ratio to counter hippocampal hyperactivity, Neuron (2023), https://doi.org/10.1016/j.neuron.2023.01.018

Neuron

CellPress
OPEN ACCESS

Article

Cannabidiol modulates excitatory-inhibitory ratio to counter hippocampal hyperactivity

Evan C. Rosenberg,[1] Simon Chamberland,[1] Michael Bazelot,[6,9] Erica R. Nebet,[1] Xiaohan Wang,[1] Sam McKenzie,[1] Swati Jain,[3,8] Stuart Greenhill,[7] Max Wilson,[7] Nicole Marley,[7] Alejandro Salah,[1] Shanice Bailey,[6] Pabitra Hriday Patra,[6] Rebecca Rose,[4] Nicolas Chenouard,[1] Simón(e) D. Sun,[1] Drew Jones,[5] György Buzsáki,[1] Orrin Devinsky,[2] Gavin Woodhall,[7] Helen E. Scharfman,[3,8] Benjamin J. Whalley,[6,9] and Richard W. Tsien[1,2,10,*]

[1]Department of Neuroscience & Physiology and Neuroscience Institute, NYU Langone Medical Center, 435 E 30th St, New York, NY 10016, USA
[2]Department of Neurology, NYU Langone Medical Center, 435 E 30th St, New York, NY 10016, USA
[3]Departments of Child and Adolescent Psychiatry, Neuroscience & Physiology, and Psychiatry, NYU Langone Medical Center, 435 E 30th St, New York, NY 10016, USA
[4]Department of Advanced Research Technologies, NYU Langone Medical Center, 435 E 30th St, New York, NY 10016, USA
[5]Department of Biochemistry and Molecular Pharmacology, NYU Langone Medical Center, 435 E 30th St, New York, NY 10016, USA
[6]School of Chemistry, Food and Nutritional Sciences, and Pharmacy, University of Reading, Hopkins Life Science Building, Whiteknights, Reading, Berks RG6 6AP, UK
[7]Aston Neuroscience Institute, School of Life and Health Sciences, Aston University, Birmingham, UK
[8]Center for Dementia Research, Nathan Kline Institute for Psychiatric Research, 140 Old Orangeburg Road, Bldg. 35, Orangeburg, NY 10962, USA
[9]GW Research Ltd, Histon, Cambridge, UK
[10]Lead contact
*Correspondence: richard.tsien@nyulangone.org
https://doi.org/10.1016/j.neuron.2023.01.018

SUMMARY

Cannabidiol (CBD), a non-euphoric component of cannabis, reduces seizures in multiple forms of pediatric epilepsies, but the mechanism(s) of anti-seizure action remain unclear. In one leading model, CBD acts at glutamatergic axon terminals, blocking the pro-excitatory actions of an endogenous membrane phospholipid, lysophosphatidylinositol (LPI), at the G-protein-coupled receptor GPR55. However, the impact of LPI-GPR55 signaling at inhibitory synapses and in epileptogenesis remains underexplored. We found that LPI transiently increased hippocampal CA3-CA1 excitatory presynaptic release probability and evoked synaptic strength in WT mice, while attenuating inhibitory postsynaptic strength by decreasing $GABA_AR\gamma_2$ and gephyrin puncta. LPI effects at excitatory and inhibitory synapses were eliminated by CBD pre-treatment and absent after GPR55 deletion. Acute pentylenetrazole-induced seizures elevated GPR55 and LPI levels, and chronic lithium-pilocarpine-induced epileptogenesis potentiated LPI's pro-excitatory effects. We propose that CBD exerts potential anti-seizure effects by blocking LPI's synaptic effects and dampening hyperexcitability.

INTRODUCTION

Neuronal circuits require coordination between synaptic excitation (E) and inhibition (I) for proper function,[1,2] and disruptions in the excitatory-to-inhibitory (E:I) ratio contribute to epilepsy,[3] autism spectrum disorders,[4] and schizophrenia.[5] G-protein-coupled receptors (GPCRs) tightly regulate the E:I ratio by linking agonists such as endocannabinoids (eCBs) to downstream signaling.[6,7] However, the exact nature of GPCR signaling often remains obscure. Understanding how GPCR agonists and antagonists influence these receptors, their downstream signaling pathways, and effector mechanisms would help clarify how CNS circuits are modulated.

(−)-*trans*-cannabidiol (CBD), a major non-euphoric component in cannabis, can reduce seizure activity in multiple animal models[8] and in patients with treatment-resistant epilepsies. Efficacy in double-blind, placebo-controlled phase III clinical trials in Dravet syndrome,[9–11] Lennox-Gastaut syndrome,[12] and tuberous sclerosis[13] led to FDA approval of highly purified, plant-derived CBD (Epidiolex in the US) for these disorders. In preclinical models, CBD reduces spontaneous recurrent seizures[14] and regulates the E:I ratio in acute seizures[15,16]; however, the molecular signaling underlying CBD's anti-seizure actions remains poorly defined.[17]

Possible therapeutic targets of CBD encompass ion channels, transporters, and transmembrane signaling proteins.[18] Among proposed candidates are two GPCRs: the cannabinoid receptor CB_1R[19,20] and de-orphanized receptor GPR55.[21,22] CBD is proposed to act as a negative allosteric modulator of CB_1R[19,20]; however, the clinical relevance of this target remains uncertain,

Please cite this article in press as: Rosenberg et al., Cannabidiol modulates excitatory-inhibitory ratio to counter hippocampal hyperactivity, Neuron (2023), https://doi.org/10.1016/j.neuron.2023.01.018

as CB_1R antagonists are proconvulsive in most preclinical models.[8]

CBD also acts a GPR55 antagonist, blocking the effects of the lipid lysophosphatidylinositol (LPI), an endogenous GPR55 agonist.[21,23] LPI drives GPR55-mediated Ca^{2+} flux at neuronal cell bodies[24] and presynaptic hippocampal CA3-CA1 (*cornu ammonis*) excitatory terminals,[20] producing an overall pro-excitatory effect. CBD blocks LPI-mediated presynaptic Ca^{2+} rises, preventing elevated glutamate release.[22] LPI effects were abolished in GPR55 KO mice, suggesting agonist-receptor selectivity.[22] Further, a synthetic GPR55 inverse agonist occluded CBD action.[15,16] These observations implicate GPR55 as a substrate for some of CBD's anti-seizure actions.

However, these studies leave many questions unanswered. Does CBD act on multiple neuronal types and, if so, how do these responses converge to affect excitability? Does CBD affect intrinsic excitability, and is synaptic strength altered pre- or postsynaptically? How do cellular mechanism(s) impact spike transmission in circuits, and how does signaling change after repeated seizures and chronic epilepsy?

To address these questions, we focused on the LPI-GPR55 signaling pathway as a potential modulator of E:I ratio and anti-seizure target of CBD. We found that LPI triggers a GPR55-dependent dual mechanism to elevate network excitability: a transient elevation in presynaptic excitatory release probability,[22] complemented by a slower sustained reduction of inhibitory synaptic strength. Downregulation of postsynaptic $GABA_A$ receptors and gephyrin scaffolding drives attenuation of synaptic inhibition. Both LPI-mediated effects on synaptic transmission were blocked by GPR55 deletion or CBD pre-treatment. Acute seizures upregulated GPR55 expression and LPI production, strongly potentiating their combined pro-excitatory effects. Our observations suggest a positive feedback loop whereby LPI promotes hyperexcitability, which in turn increases the expression of LPI and GPR55. We propose LPI-GPR55 signaling as a potential target for CBD in reducing seizures, complementary to the direct effects of CBD on ion channels.[15,16,25–27]

RESULTS

Hippocampal GPR55 expression and LPI enhancement of spike throughput

We studied mechanisms of CBD action in the hippocampus, a key driver of temporal lobe seizures.[28] GPR55 was strongly expressed in hippocampal CA1 and CA3 pyramidal layers derived from male wild-type (WT) C57BL/6J mice, with lower expression in CA2 and the dentate gyrus (DG) granule layer (Figures 1A and 1B; $p_{CA1/CA2}$ = 0.033, $p_{CA1/DG}$ = 0.0002, $p_{CA3/DG}$ = 0.0006). Punctate GPR55 labeling also occurred in the CA1 *stratum radiatum* (S.R.), consistent with incoming CA3 Schaffer collateral axon terminals[22] (Figure S3A), although glial and postsynaptic expression cannot be excluded. Anti-GPR55 antibody labeling was greatly reduced in GPR55 KO mice (male *B6;129S-Gpr55^{tm1Lex}/Mmnc*), seen at low (10×) and high (63×) magnification (Figures 1A and 1B; $p < 0.0001$ for all regions), demonstrating antibody specificity. Thus, GPR55 is well-expressed at CA3 to CA1 inputs, supporting its role in regulating synaptic strength.

GPR55 is implicated in the seizure-reducing properties of CBD

To investigate GPR55 as a potential target for the anticonvulsant effects of CBD, we first studied an *in vivo* model of acute, generalized seizures in mice, using pentylenetetrazole (PTZ, 105 mg/kg, intraperitoneally [i.p.]) (Figure 1C). Administration of CBD (50, 100, 200 mg/kg, i.p., 1 h prior to PTZ injection)[29] produced a dose-dependent reduction in tonic-clonic seizures, reaching significance at 200 mg/kg, i.p. (n_{WT+VEH} = 18/18 vs. n_{WT+CBD} = 5/15, $p < 0.0001$). In contrast, the seizure-reducing effects of CBD were absent in GPR55 KO mice, even at 200 mg/kg (n_{KO+VEH} = 11/13 vs. n_{KO+CBD} = 10/13 KO, $p > 0.9999$). At 200 mg/kg, significantly more GPR55 KO mice had tonic-clonic seizures than WT mice ($p = 0.03$). Thus, dampening of behavioral seizures appeared to be GPR55-dependent.

CBD reduced mortality both in WT (Figure 1D; n_{WT+VEH} = 16/18 death vs. n_{WT+CBD} = 0/15, $p < 0.0001$) and KO mice (n_{KO+VEH} = 10/13 vs. n_{KO+CBD} = 0/13 KO, $p = 0.0001$), suggesting a potential GPR55-independent effect of CBD. To confirm that we did not miss covert electrographic seizures that contributed to mortality, we performed tungsten electrode recordings from CA1 and verified that electrographic seizure activity correlated with behavioral assays in WT (n = 3) and GPR55 KO (n = 3) genotypes (Figures S1A–S1C). Overall, these results suggested that GPR55 might play a key role in CBD's anticonvulsive effects, but potentially not seizure-induced mortality, prompting further study of CBD and GPR55 interaction.

The striking effects of deleting the GPR55 receptor suggest that its endogenous agonist, LPI, promotes seizure-like activity.[22] To explore this, we tested LPI's effect on synaptically driven excitation at the CA3→CA1 (Schaffer collateral) input. Exposure to LPI transiently increased spike probability (Figure 1E; $p = 0.038$). This enhancement of excitation-spike coupling (Figure 1F) was prevented by 1 μM CBD pre-treatment (p_{ANOVA} = 0.017, $p_{LPI/LPI+CBD}$ = 0.025) and absent in slices from GPR55 KO mice ($p_{LPI\text{-}WT/LPI\text{-}KO}$ = 0.021; Figure S1D; Table S1). Exposing hippocampal slices to LPI (4 μM) did not change the intrinsic frequency-current (F-I) relation (Figure 1G, n = 6) or spontaneous firing rate of CA1 pyramidal cells (Figure 1H; Figure S1E; $p = 0.74$). Therefore, we predict that LPI elevates synaptic drive in a CBD- and GPR55-dependent manner, without affecting pyramidal cell intrinsic firing.

CBD blocks the pro-excitatory and dis-inhibitory effects of LPI

Feedforward CA3→CA1 signaling depends on both monosynaptic excitation (E→E) and disynaptic feedforward inhibition (E→I→E), prompting the examination of LPI's effects at each part of the microcircuit. In excitatory boutons, LPI releases Ca^{2+} from presynaptic stores and transiently enhances glutamatergic transmission in a GPR55-dependent and CBD-sensitive manner.[22] We confirmed that LPI (4 μM) enhanced spontaneous neurotransmission, reflected by increased miniature excitatory postsynaptic current (mEPSC) frequency in CA1 pyramidal neurons (Figures $2A_1$–$2C_1$; Figure S2A; p_{Freq} = 0.0001), without changes in mEPSC amplitude (p_{Ampl} = 0.30). Miniature inhibitory postsynaptic currents (mIPSCs) recorded at V_{rest} in 1 μM tetrodotoxin (TTX) were unchanged immediately following LPI

Please cite this article in press as: Rosenberg et al., Cannabidiol modulates excitatory-inhibitory ratio to counter hippocampal hyperactivity, Neuron (2023), https://doi.org/10.1016/j.neuron.2023.01.018

CellPress
OPEN ACCESS

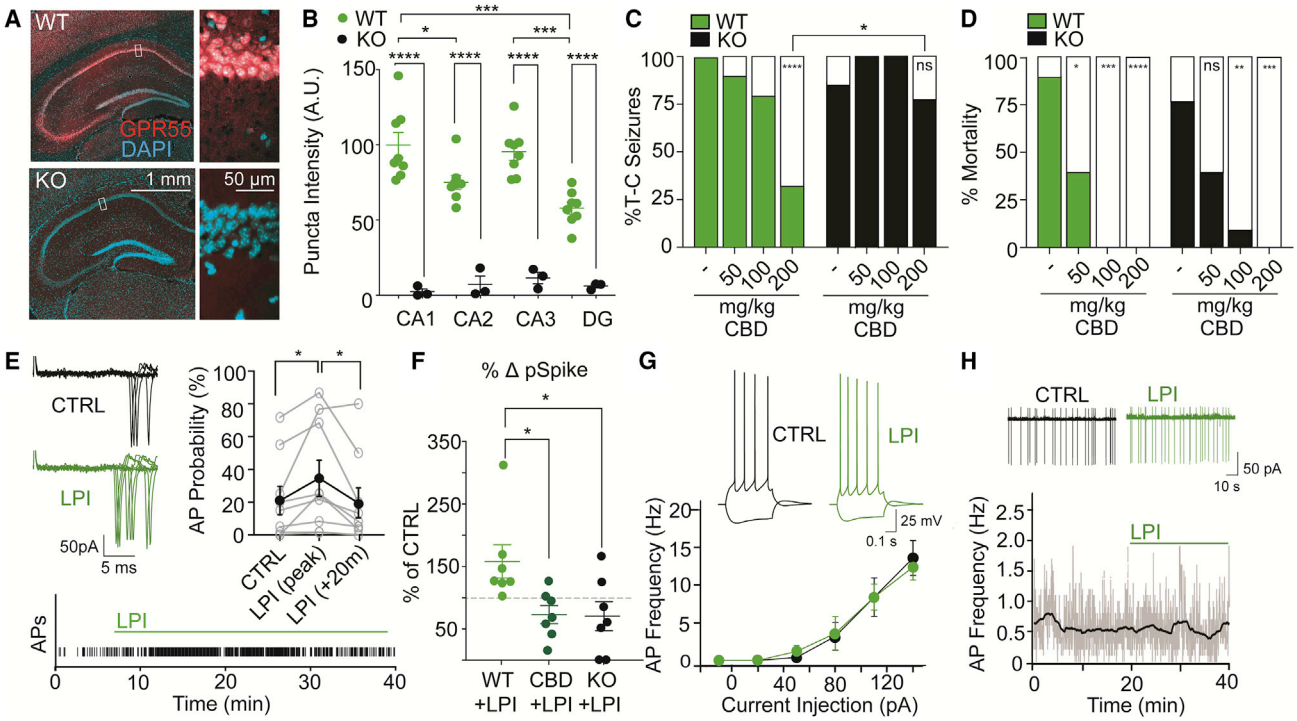

Figure 1. CBD reduces seizures and LPI-driven CA3→CA1 spike enhancement via GPR55

(A) GPR55 expression in hippocampal slices (10×, 63× resolution) is absent in slices from the GPR55 KO mouse.

(B) GPR55 expression (20×) was greater in the pyramidal layer of area CA1 and CA3 than the pyramidal layer of CA2 or granule layer of DG (n_{WT} = 8 slices, $p_{CA1/CA2}$ = 0.033, $p_{CA1/DG}$ = 0.0002, $p_{CA3/DG}$ = 0.0006). GPR55 expression was significantly reduced in all regions in control slices from GPR55 KO littermates (n_{KO} = 3, $p < 0.0001$ for all regions).

(C) CBD produced dose-dependent reduction in seizures generated by pentylenetetrazole (PTZ, 105 mg/kg): significant effects at 200 mg/kg, i.p. (n_{WT+VEH} = 18/18 vs. $n_{WT+CBD200}$ = 5/15, $p < 0.0001$). However, CBD did not reduce PTZ-induced seizures in GPR55 KO mice (n_{KO+VEH} = 11/13 vs. $n_{KO+CBD200}$ = 10/13 KO, $p_{KO+VEH/KO+CBD200} > 0.9999$; $p_{WT+CBD200/KO+CBD200}$ = 0.03).

(D) CBD decreased mortality in PTZ-induced seizures in both WT ($p_{WT+VEH/WT+CBD50}$ = 0.011, $p_{WT+VEH/WT+CBD100}$ = 0.0008, $p_{WT+VEH/WT+CBD200} < 0.0001$) and GPR55 KO mice ($p_{KO+VEH/KO+CBD100}$ = 0.0028, $p_{KO+VEH/KO+CBD200}$ = 0.0001).

(E and F) In cell-attached recordings, LPI transiently elevated the probability of evoking an action potential with Schaffer collateral stimulation (5× 50 Hz at 5 s intervals) (n = 9, p = 0.038), an effect that decayed by 20 min following LPI onset (p = 0.034 vs. peak). The LPI-induced effect was blocked by 1 µM CBD pre-treatment ($n_{LPI+CBD}$ = 7, p_{ANOVA} = 0.017, $p_{LPI/LPI+CBD}$ = 0.025) and absent in GPR55 KO slices ($n_{LPI-WT/LPI-KO}$ = 7, $p_{LPI-WT/LPI-KO}$ = 0.021).

(G and H) (G) The frequency-current (F-I) relationship and (H) cell-attached spontaneous firing rate of CA1 pyramidal neurons remain unchanged upon LPI (4 µM) addition (n = 6, p = 0.74). Throughout, symbols and error bars represent mean of independent samples ± standard error of mean; *p ≤ 0.05, **p ≤ 0.01, ***p ≤ 0.001, ****p < 0.0001.

application (Figure 2 legend), but after 20–30 min LPI exposure, decreased substantially in frequency and amplitude (Figures 2A_2–2C_2). The decreased mIPSC rate (Figures 2A_2–2C_2; Figures S2C and S2D; p_{Freq} = 0.0002) and size (p_{Ampl} = 0.0003) were reversed by removing LPI (Figure 2B_2; Figure S2D).

CBD without LPI did not alter baseline mEPSC frequency (Figure 2B_1; p_{Freq} = 0.51). However, 1 µM CBD pre-treatment eliminated the pro-excitatory effects of LPI (Figures 2A_1–2C_1: p_{Freq} = 0.82). Likewise, 1 µM CBD without LPI did not change mIPSC frequency (Figure 2B_2; p_{Freq} = 0.65 vs. baseline) or amplitude (p_{Ampl} = 0.94), but prevented the LPI-mediated decreases in mIPSC frequency and amplitude (Figures 2A_2–2C_2; p_{Freq} = 0.97 vs. baseline; p_{Ampl} = 0.32).

GPR55 receptor deletion eliminated the pro-excitatory and anti-inhibitory effects induced by LPI (Figure 2, black traces; Figure S2). Slices from GPR55 KO mice showed neither an LPI-mediated increase in mEPSC frequency (p_{Freq} = 0.54 vs. baseline) nor LPI-driven reductions in mIPSC frequency (p_{Freq} = 0.47) and amplitude (p_{Ampl} = 0.19). Thus, GPR55 KO had the same effect as CBD in most aspects of unitary synaptic transmission. A possible exception was basal mEPSC amplitude (Figure S2A), which appeared slightly larger in neurons from GPR55 KO mice (black, 26 ± 1 pA) than in WT (green, 22 ± 1 pA, p_{Ampl} = 0.018), suggesting that GPR55 receptor deletion could have a developmental effect on excitatory synapses.[30] In contrast, the basal mIPSC amplitude (Figure S2C) was similar in GPR55 KO and WT recordings (p = 0.37).

We next asked whether CB_1Rs modulate LPI signaling through colocalization and heterodimerization with GPR55.[31]We tested this using an antagonist of CB_1Rs, AM281, with minimal activity at GPR55 at 1 µM.[23] However, LPI's effects on excitatory and inhibitory transmission remained robust, with 1 µM AM281 (Figure 2C_1; $p_{mEPSC\text{-}Freq}$ = 0.048, aligned with prior studies[22]; Figure 2C_2, $p_{mIPSC\text{-}Freq}$ = 0.034; $p_{mIPSC\text{-}Ampl}$ = 0.016) weighing

Please cite this article in press as: Rosenberg et al., Cannabidiol modulates excitatory-inhibitory ratio to counter hippocampal hyperactivity, Neuron (2023), https://doi.org/10.1016/j.neuron.2023.01.018

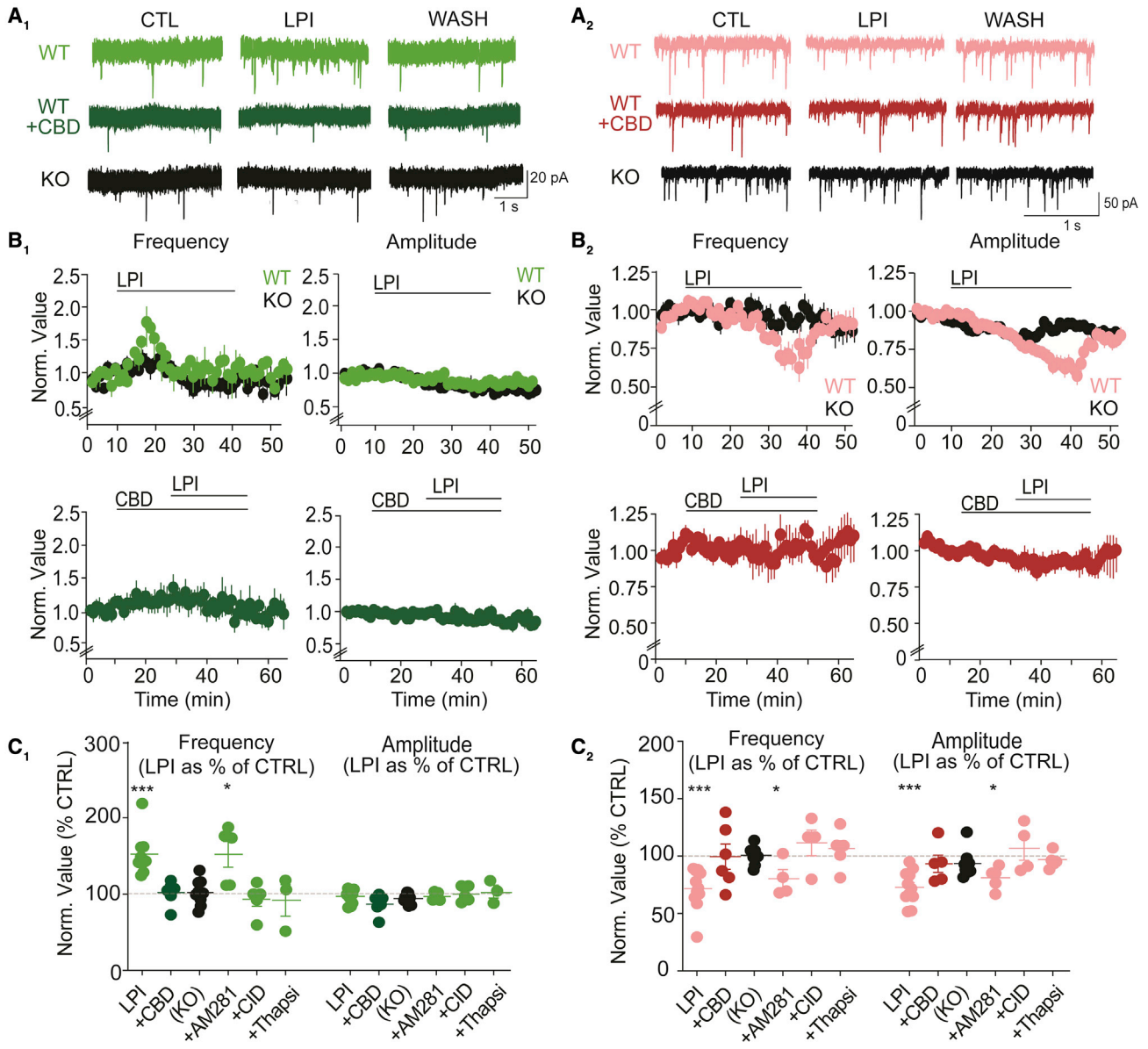

Figure 2. CBD blocks both pro-excitatory and anti-inhibitory effects of LPI

(A) (A_1 and A_2) Representative electrophysiological traces of spontaneous synaptic transmission. LPI (4 μM) reversibly elevated mEPSC frequency, without changing mEPSC amplitude (A_1, light green traces). Contrarily, LPI diminished both the frequency and the amplitude of mIPSCs, reversed by wash (A_2, pink traces). CBD pre-treatment (1 μM) prevented LPI-mediated increases in mEPSC frequency (A_1, dark green) and LPI-driven decreases in mIPSC amplitude and frequency (A_2, red). Additionally, LPI effects were absent in slices from GPR55 KO mice (A_1 and A_2, black traces).

(B) (B_1 and B_2) Time courses of LPI-mediated effects: transient rise in mEPSC frequency (~5 min to peak, light green, upper panel, left) and slow, gradual reduction in mIPSC frequency and amplitude (20–30 min, pink, upper panels, right), absent in slices from GPR55 KO mice (black symbols, rear) and prevented by CBD pre-treatment (B_1, dark green, mEPSCs; B_2, mIPSCs red).

(C) (C_1 and C_2) Effect of LPI to both elevate mEPSC frequency (left, C_1, n = 10, p = 0.0001 vs. baseline), and lower mIPSC frequency (right, C_2, n = 10, p = 0.0002) and amplitude (p = 0.0003), was absent following CBD application (dark green, n = 6, C_1; red, n = 5, C_2) and ablated in GPR55 KO mice (black, n_{mEPSC} = 9, n_{mIPSC} = 8). However, effects persisted in the presence of the CB_1R antagonist AM281 (1 μM) (n_{mEPSC} = 5, p_{mEPSC} = 0.048, n_{mIPSC} = 4, $p_{mIPSC\text{-}Freq}$ = 0.034; $p_{mIPSC\text{-}Ampl}$ = 0.016). LPI-mediated changes also blocked by the synthetic GPR55 inverse agonist CID16020046 (CID, 2.5 μM, n_{mEPSC} = 5, p_{mEPSC} = 0.10; n_{mIPSC} = 4, $p_{mIPSC\text{-}Freq}$ = 0.44; $p_{mIPSC\text{-}Ampl}$ = 0.52) and the SERCA pump inhibitor thapsigargin (Thapsi, 10 μM, n_{mEPSC} = 3, p_{mEPSC} = 0.76; n_{mIPSC} = 5, $p_{mIPSC\text{-}Freq}$ = 0.58; $p_{mIPSC\text{-}Ampl}$ = 0.44).

Please cite this article in press as: Rosenberg et al., Cannabidiol modulates excitatory-inhibitory ratio to counter hippocampal hyperactivity, Neuron (2023), https://doi.org/10.1016/j.neuron.2023.01.018

against LPI action via CB_1Rs. Because CBD has multiple non-GPR55 targets,[18] we evaluated a role for GPR55 using the synthetic GPR55-selective inverse agonist CID16020046 (Figure 2C_1). Pre-treatment of slices with CID16020046 (2.5 μM) abolished the LPI-induced elevation of mEPSC frequency ($p = 0.10$) and prevented the anti-inhibitory effect of LPI on mIPSC frequency (Figure 2C_2; $p = 0.44$) and amplitude ($p = 0.52$).

Although the pro-excitatory and anti-inhibitory effects of LPI had different time courses, both effects might rely on the GPR55-mediated discharge of intracellular calcium stores. Accordingly, we pre-depleted Ca^{2+} stores via thapsigargin (10 μM), which completely blocked the LPI-induced responses (Figures 2C_1 and 2C_2), including mEPSC frequency ($p = 0.76$ vs. baseline), mIPSC frequency ($p = 0.58$), and mIPSC amplitude ($p = 0.44$). Therefore, LPI acts through CBD-sensitive GPR55 receptors to release intracellular Ca^{2+} and thereby modify excitatory[22] and inhibitory synapses.

We used Ca^{2+} imaging to assess the effects of LPI on critical Ca^{2+} stores. Because LPI does not increase mIPSC frequency (Figure 2B_2), we predicted that LPI might affect Ca^{2+} stores in inhibitory presynaptic boutons differently than excitatory terminals.[22] Presynaptic Ca^{2+} regulation in GABAergic terminals in GCaMP6f-expressing parvalbumin-positive (PV+) interneurons (male PV-Cre × Ai148 mice) was assayed with two-photon Ca^{2+} imaging, focusing on presynaptic terminals innervating CA1 pyramidal cell bodies. Presynaptic Ca^{2+} in the GABAergic terminals was unaffected by LPI (4 μM, 3 min), yet reliably elevated by [K]-rich solution (Figure S2E). Thus, inhibitory and excitatory presynaptic terminals differ: LPI failed to discharge inhibitory presynaptic Ca^{2+} stores, suggesting that it might act postsynaptically.[22,24]

GPR55 expression at excitatory and inhibitory synapses

Given the differing effects of LPI on excitatory and inhibitory synaptic transmission, we used immunohistochemistry (IHC) and immunocytochemistry (ICC) on hippocampal slices (Figure S3A) to assess the colocalization of GPR55 with presynaptic and postsynaptic markers: for excitatory synapses, vesicular glutamate transporter 1 (VGLUT1) and postsynaptic density protein (PSD-95); for inhibitory synapses, vesicular GABA transporter (VGAT) and postsynaptic Gephyrin. GPR55 puncta colocalized more strongly with VGLUT1 than with the inhibitory presynaptic marker VGAT in both S.R. and *stratum pyramidale* (S.P.) (Figure S3A; $p_{S.R.} = 0.044$, $p_{S.P.} = 0.020$) and much more strongly with Gephyrin than VGAT ($p_{S.R.} = 0.014$, $p_{S.P.} = 0.027$). These observations suggest that GPR55 has a greater expression at postsynaptic inhibitory sites than inhibitory axon terminals, providing a rationale for the absence of LPI's effects on Ca^{2+} transients in presynaptic GABAergic terminals (Figure S2E). However, these colocalization analyses are limited to the spatial resolution imposed by three-dimensional light microscopy (~200 nm XY).

For better spatial visualization and less background fluorescence, we examined GPR55 localization at hippocampal synapses in dissociated cell cultures, using high-resolution confocal microscopy and demonstrated antibody specificity (Figure S3B). Cell culture studies reflected patterns seen in acute slice (Figures S3C–S3G). To exclude colocalization by chance alone, we scrambled GPR55 pixel locations along a 2D axon and compared colocalization levels to non-randomized conditions (Figure S3G; STAR Methods). GPR55 colocalized better than chance with VGLUT1 ($p = 0.0002$), PSD-95 ($p < 0.0001$), and Gephyrin ($p < 0.0001$), but not VGAT ($p = 0.93$). Thus, GPR55 colocalizes with excitatory synaptic markers and postsynaptic inhibitory markers, in line with the effects of GPR55 ligands on synaptic function.

We examined potential colocalization of GPR55 and CB_1Rs,[32] which are presynaptically localized, sensitive to cannabinoids, and regulators of synaptic activity.[33] CB_1R can heterodimerize with GPR55 to reciprocally regulate cannabinoid signaling.[31] CB_1R and GPR55 expression appeared to alternate along a single axon (Figure S3E, linescan), with rare colocalization (Figures S3A, S3E, and S3G) that was greater than chance alone (Figure S3G; $p = 0.0061$). Thus, GPR55 and CB_1R largely occupy complementary domains along an axon but might occasionally colocalize or heterodimerize.

LPI modulates evoked transmission, enhancing excitation and reducing inhibition

After establishing that LPI modulates unitary synaptic currents via synaptic GPR55, we studied spike-evoked transmission in the CA3→CA1 microcircuit, recording from CA1 pyramidal neurons while stimulating Schaffer collateral axons in S.R. (Figure 3A_1, 10 × 10 Hz). Inward excitatory currents were isolated in whole-cell voltage clamp recordings with cells held at E_{Cl} (~−70 mV) to eliminate GABAergic IPSCs. Exposure to LPI (4 μM) caused a reversible 22% ± 6% elevation in the evoked EPSC amplitude during a 5 min window beginning 5 min post-LPI application onset (Figures 3A_1–3A_3; $p_{LPI/baseline} = 0.021$). Concurrently, the paired pulse ratio (PPR), the ratio of amplitudes of second- and first-evoked EPSCs, fell by 17% ± 3% ($p_{LPI/baseline} = 0.0092$). Together, these effects suggest that LPI transiently elevates the probability of evoked excitatory transmitter release, consistent with observations that LPI elevates mEPSC frequency[22] (Figure 2B_1), field EPSP strength,[22] and long-term potentiation.[34] Pre-treatment with 1 μM CBD prevented the increased eEPSC amplitude ($p_{ANOVA} = 0.0078$: $p_{LPI/CBD+LPI} = 0.0057$) and the reduced PPR ($p_{ANOVA} = 0.036$: $p_{LPI/CBD+LPI} = 0.042$) (Figure 3A_3; Figure S4; Table S1). GPR55 deletion acted similarly (Figure 3A_3; Figure S4): eliminating LPI-driven changes in eEPSC amplitude ($p_{WT/KO} = 0.028$) and in PPR ($p_{WT/KO} = 0.048$; Table S1).

We next asked how LPI affects disynaptic feedforward inhibition in CA1 (CA3-derived inputs→ interneurons→ CA1 pyramidal cells). Inhibitory synaptic currents (evoked IPSCs, eIPSCs) were isolated by holding CA1 pyramidal cells at the reversal potential EPSCs (E_{exc} = ~0 mV), stimulating Schaffer collaterals, and recording outward GABAergic currents (Figure 3B_1, 10 × 10 Hz). Application of glutamatergic synaptic blockers (10 μM NBQX, 2,3-dihydroxy-6-nitro-7-sulfamoyl-benzo[f]quinoxaline, and 50 μM APV, 2-amino-5-phosphonopentanoate) abolished eIPSCs, confirming that outward eIPSCs were disynaptic (Figure S4C; $p = 0.0051$). After 25 min of exposure, LPI reduced eIPSC amplitude by 60%–70% (Figures 3B_1–3B_3; $p_{LPI/baseline} = 0.0006$), while dramatically elevating the eIPSC PPR ($p_{LPI/baseline} = 0.039$). The LPI-mediated decrease in eIPSC

Please cite this article in press as: Rosenberg et al., Cannabidiol modulates excitatory-inhibitory ratio to counter hippocampal hyperactivity, Neuron (2023), https://doi.org/10.1016/j.neuron.2023.01.018

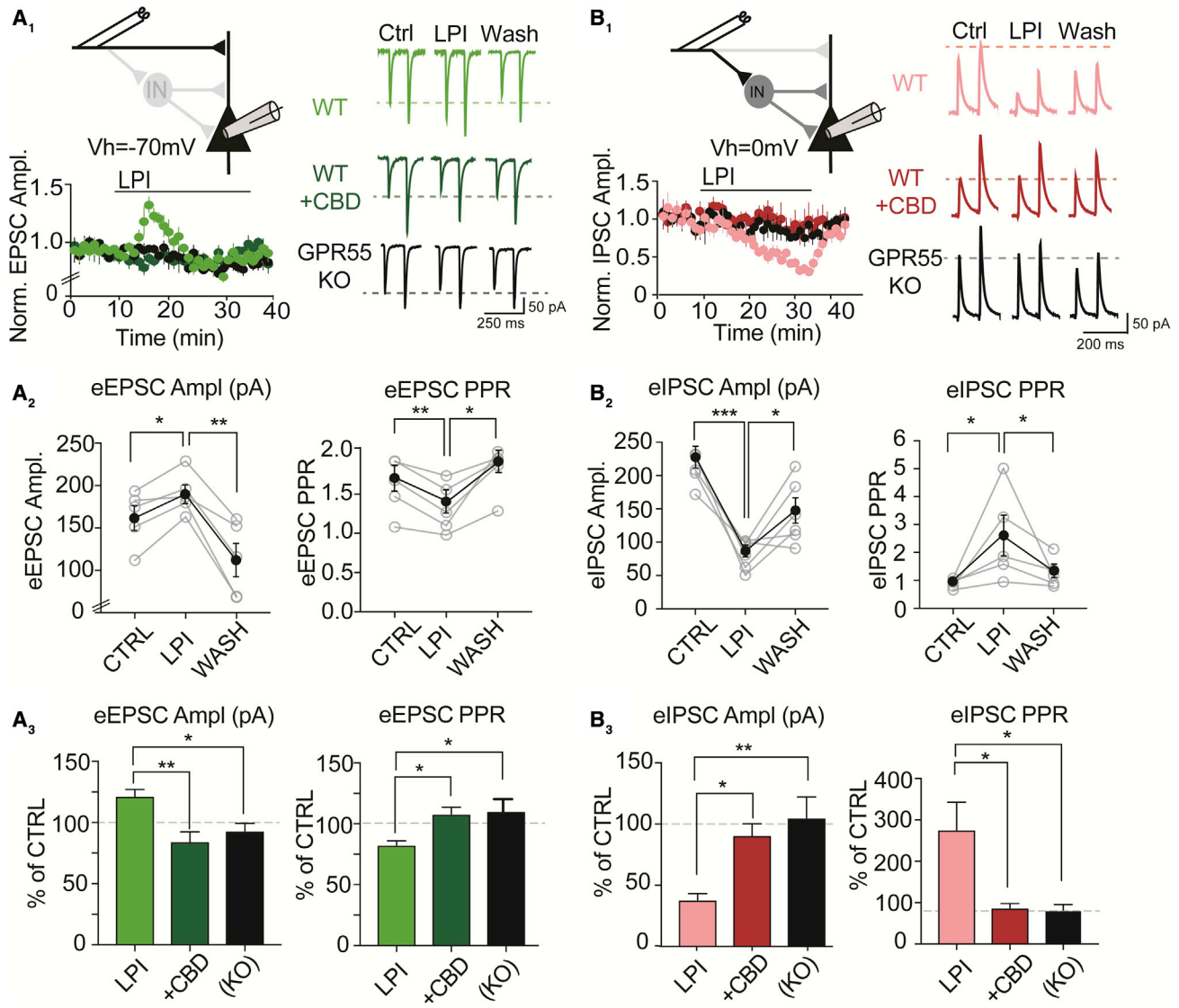

Figure 3. LPI regulates synaptically evoked transmission in the CA3→CA1 microcircuit by augmenting excitation and diminishing disynaptic inhibition

(A) (A_1) CA1 pyramidal neuron recordings (V_{hold} = −70 mV), with stimulating electrodes placed in *stratum radiatum* to activate Schaffer collateral axons. LPI (4 μM) caused a transient, reversible elevation in synaptically evoked EPSCs (eEPSCs) in WT (light green) slices, blocked by CBD pre-treatment (dark green) and absent in GPR55 KO slices (black). (A_2 and A_3) LPI elevated eEPSC amplitude (n_{LPI} = 5, $p_{LPI/baseline}$ = 0.021, 5 min window, 5 min post-LPI application), corresponding to a drop in the paired pulse ratio (PPR) of second vs. first events ($p_{LPI/baseline}$ = 0.0092, $p_{LPI/Wash}$ = 0.020). Both LPI-mediated effects were blocked by 1 μM CBD (Ampl: $n_{CBD+LPI}$ = 5, p_{ANOVA} = 0.0078, $p_{LPI/CBD+LPI}$ = 0.0057; PPR: p_{ANOVA} = 0.036, $p_{LPI/CBD+LPI}$ = 0.042) and deficient in GPR55 KO mice (Ampl: n_{KO} = 5, $p_{WT/KO}$ = 0.028; PPR: $p_{WT/KO}$ = 0.048).

(B) (B_1–B_3) Effects on disynaptic inhibitory currents isolated by holding CA1 neurons at 0 mV (~E_{Glu}), (Figure S4C) (B_1) LPI gradually reduced eIPSC amplitude (pink), an effect prevented by CBD pre-treatment (red) and deficient in GPR55 KO slices (black). (B_2 and B_3) eIPSC amplitude lowered by application of LPI (n = 6, $p_{LPI/baseline}$ = 0.0006, 5 min window, 25 min post LPI). LPI reversibly elevated PPR over the same time intervals ($p_{LPI/baseline}$ = 0.039). LPI-mediated effects were prevented by CBD pre-treatment (Ampl: $n_{CBD+LPI}$ = 4, p_{ANOVA} = 0.0022, $p_{LPI/CBD+LPI}$ = 0.014; PPR: $p_{LPI/CBD+LPI}$ = 0.021) and absent in GPR55 KO slices (Ampl: n_{KO} = 5, $p_{WT/KO}$ = 0.0018; PPR: $p_{WT/KO}$ = 0.013).

amplitude was prevented by 1 μM CBD (Figure 3B_3; Figure S4D; Table S1; p_{ANOVA} = 0.0022: $p_{LPI/CBD+LPI}$ = 0.014) and absent in GPR55 KO slices ($p_{WT/KO}$ = 0.0018). Similarly, the elevated eIPSC PPR was blocked by CBD ($p_{LPI/CBD+LPI}$ = 0.021) and not apparent in GPR55 KO slices ($p_{WT/KO}$ = 0.013). The temporal disparity between early transient elevation of EPSC amplitude (Figure 3A_1) and slowly developing attenuation of IPSC amplitude (Figure 3B_1) resembled the contrasting kinetics of changes in mEPSC frequency (Figure 2B_1) and mIPSC amplitude (Figure 2B_2). A similar pattern was evident in compound (E+I) synaptic currents (n = 9, Figure S4A), with an early elevation in E:I ratio that persisted following LPI washout (Figure S4A).

Please cite this article in press as: Rosenberg et al., Cannabidiol modulates excitatory-inhibitory ratio to counter hippocampal hyperactivity, Neuron (2023), https://doi.org/10.1016/j.neuron.2023.01.018

CellPress
OPEN ACCESS

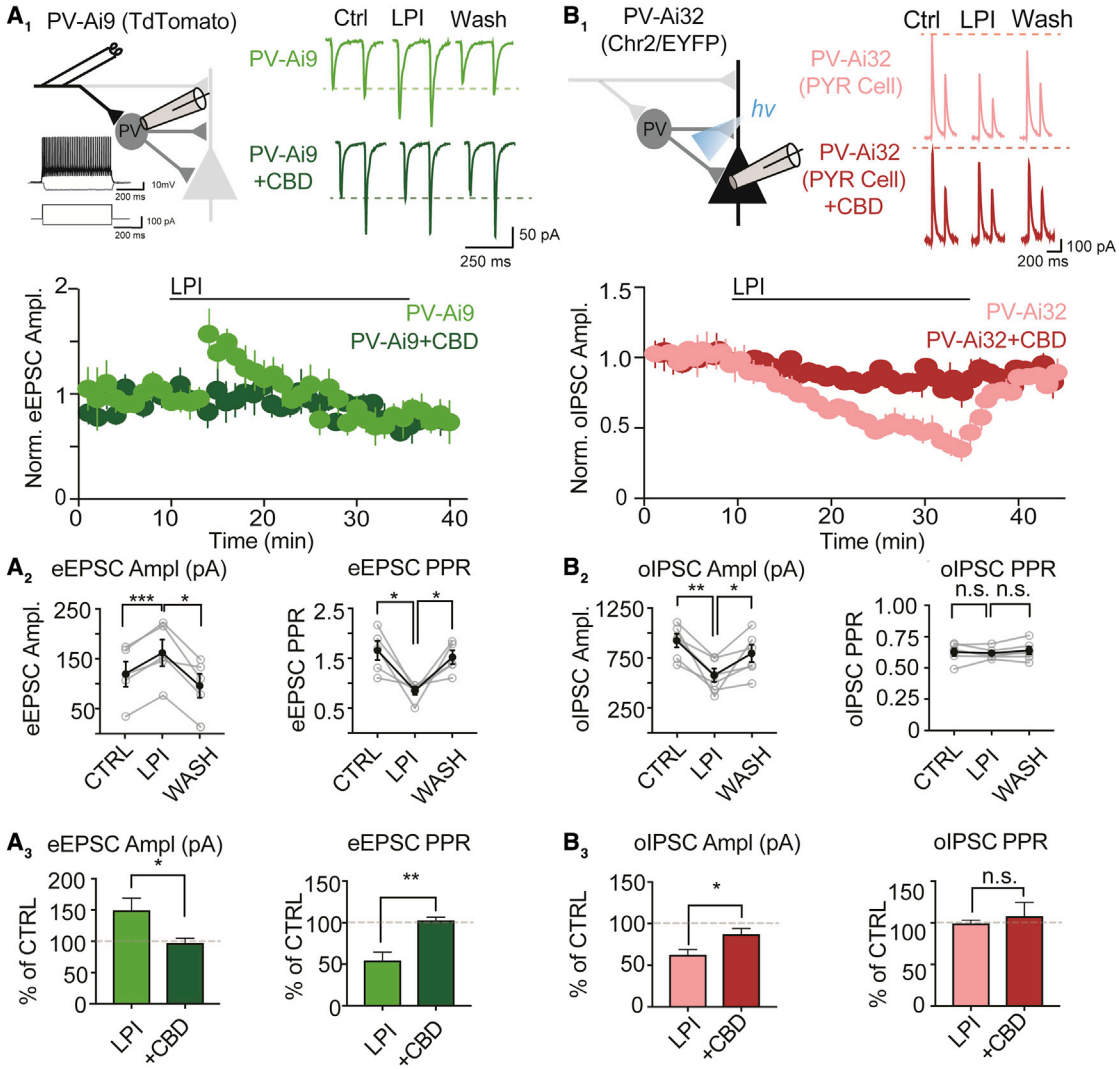

Figure 4. LPI transiently strengthens PV neuron inputs while persistently weakening their inhibitory output

(A) (A_1–A_3) Recording in genetically labeled PV-Cre × Ai9 interneurons. LPI (4 μM)-elevated Schaffer collateral-evoked (e) EPSC amplitude (light green, n = 5, $p_{LPI/baseline}$ = 0.0007), reverted during wash ($p_{LPI/Wash}$ = 0.012). Concurrently, LPI reduced the PPR ($p_{LPI/baseline}$ = 0.022; $p_{LPI/Wash}$ = 0.031). CBD pre-treatment prevented effects of LPI on amplitude (dark green, $n_{CBD+LPI}$ = 5, $p_{LPI/CBD+LPI}$ = 0.035) and PPR ($p_{CBD+LPI}$ = 0.0020).

(B) (B_1–B_3) LPI reduced amplitude of optogenetically evoked monosynaptic IPSCs (oIPSCs) in slices from PV-Cre × Ai32/ChR2 mice (pink, n_{LPI} = 6, $p_{LPI/baseline}$ = 0.0052, $p_{LPI/Wash}$ = 0.039) but did not change the PPR ($p_{LPI/baseline}$ = 0.71). CBD blocked effects of LPI on IPSCs (red, p = 0.028).

LPI-CBD opposition at E→I and I→E connections along the disynaptic pathway

The strong effects of LPI and CBD on feedforward inhibition motivated us to study the modulation of individual synaptic elements in the disynaptic circuit (Figure 4), focusing on PV+ interneurons, a key relay in feedforward inhibition.[35,36] Genetically labeled CA1 S.P. PV+ neurons from male *B6;129P2-Pvalb$^{tm1(cre)Arbr}$/B6.Cg-Gt(ROSA)26Sor$^{tm9(CAG-tdTomato)Hze}$* mice displayed characteristic brief membrane time constants and high frequency spiking patterns (Figure 4A_1; Figure S5A). LPI elevated mEPSC frequency in PV+ neurons after 5 min drug exposure, but not in the presence of CBD (Figure S5B). LPI also increased Schaffer collateral-evoked EPSC amplitude (Figures 4A_1–4A_3; $p_{LPI/baseline}$ = 0.0007) and decreased the eEPSC PPR (Figure 4A_2; $p_{LPI/baseline}$ = 0.022) Notably, pre-treatment with CBD (Figure 4A_3; Figure S5D) prevented LPI from increasing eEPSC amplitude ($p_{LPI/CBD+LPI}$ = 0.035) and reducing eEPSC PPR ($p_{CBD+LPI}$ = 0.0020). Thus, LPI enhanced release probability at Schaffer collateral synapses onto PV+ interneurons, an effect abolished by CBD, in line with colocalization of GPR55 with VGLUT1 near PV+ somata (Figure S5C) and resembling E→E synaptic counterparts (Figure 3A).

To isolate the LPI effects on PV+ I→E synapses onto pyramidal neurons, we used slices from PV-Cre/Ai32/ChR2 mice expressing channelrhodopsin in PV+ terminals (Figure 4B_1, male *B6;Cg-Gt(ROSA)26Sor$^{tm32(CAG-COP4*H134R/EYFP)Hze}$/B6;129P2-Pvalb$^{tm1(cre)Arbr}$*). Blue light activation of PV fibers in the CA1 region of the hippocampus (10 × 10 Hz) caused an outward, optically evoked IPSC (oIPSC) in CA1 pyramidal cells. LPI

Please cite this article in press as: Rosenberg et al., Cannabidiol modulates excitatory-inhibitory ratio to counter hippocampal hyperactivity, Neuron (2023), https://doi.org/10.1016/j.neuron.2023.01.018

exposure (25 min) lowered monosynaptic IPSC amplitude (Figures 4B$_1$–4B$_3$; $p_{LPI/baseline}$ = 0.0052), leaving oIPSC PPR unchanged ($p_{LPI/baseline}$ = 0.71). CBD pre-treatment blocked LPI effects on oIPSC amplitude (Figure 4B$_3$; Figure S5E; n = 5 CBD + LPI, p = 0.028), also with no net effect on oIPSC PPR (Figure S5E; $p_{LPI/CBD+LPI}$ = 0.59). Thus, LPI reduces monosynaptic inhibitory transmission from PV+ interneuron to CA1 pyramids via a likely postsynaptic mechanism. However, we cannot exclude a role for LPI in regulating PV+ neuron excitability through ion channel modulation,[15,16,25–27] which could contribute to changes seen in disynaptic PPR (Figure 3B$_2$).

LPI gradually attenuates clustering of GABA$_A$R γ_2 and gephyrin at inhibitory postsynaptic sites

To clarify molecular underpinnings of LPI and CBD actions at GABAergic inhibitory synapses, we examined effects on GABA$_A$Rs, heteropentameric protein complexes trafficked to synapses via the inclusion of the γ_2 subunit[37] and anchored by the gephyrin scaffold.[38] Neuronal cultures from Sprague-Dawley rats (both sexes) were exposed to 4 μM LPI, fixed 30 and 60 min later, and imaged using MAP2 as a dendritic marker. LPI reduced the intensity of GABA$_A$R γ_2 puncta below vehicle treatment controls at both 30 min (p_{ANOVA} < 0.0001; $p_{VEH/LPI-30}$ = 0.0001) and 60 min ($p_{VEH/LPI-60}$ = 0.0003) post application (Figure 5A; Table S1). The LPI-mediated decrease in GABA$_A$R γ_2 puncta intensity reversed after 10 min ACSF washout (Figure S6A; $p_{LPI/WASH}$ = 0.014). The GABA$_A$R γ_2 puncta density per unit dendrite area was reduced at 60 min but not at 30 min post-LPI (Figure S6B; $p_{VEH/LPI-60}$ = 0.029).

Similarly, LPI diminished the intensity of gephyrin puncta at 30 (p_{ANOVA} = 0.0016; $p_{VEH/LPI-30}$ = 0.0011) and 60 min ($p_{VEH/LPI-60}$ = 0.032) post-LPI (Figure 5A; Table S1). Following a 10-min ACSF wash, gephyrin intensity overshot baseline levels (Figure S6A; $p_{LPI/WASH}$ = 0.0002, $p_{VEH/WASH}$ = 0.026). LPI reduced gephyrin puncta density only at 60 min post treatment (Figure S6B; $p_{VEH/LPI-60}$ = 0.042). LPI left the percentage of receptor puncta that were colocalized with gephyrin unchanged (Figures S6C and S6D), suggesting that gephyrin and γ_2 intensity decreased together. These data suggest that LPI diminishes both GABA$_A$Rs and their gephyrin scaffold in synaptic puncta (consistent with lowered mIPSC amplitude; Figure 2B$_2$), before reducing puncta density (thus contributing to lessened mIPSC frequency; Figure 2B$_2$).

Consistent with findings with synaptic transmission (Figure 3), CBD pre-treatment (1 μM) prevented the LPI-mediated reductions in GABA$_A$R γ_2 intensity (Figure 5A; Table S1; $p_{LPI/CBD+LPI}$ < 0.0001) and GABAR γ_2 puncta density per unit area (Figure S6E; $p_{LPI/CBD+LPI}$ = 0.0001). Furthermore, CBD blocked the LPI-driven decreases in gephyrin intensity (Figure 5A; Table S1; $p_{LPI/CBD+LPI}$ = 0.0007) and gephyrin puncta per unit area (Figure S6E; $p_{LPI/CBD+LPI}$ = 0.0005).

To test whether LPI effects on inhibitory synaptic proteins were mediated by GPR55, we transfected cell cultures with GPR55-targeted shRNA; GPR55 protein expression was significantly reduced by shRNA (Figure S6F; p = 0.034) but not in scrambled shRNA controls (p = 0.89). Knockdown of GPR55 with shRNA transfection prevented the LPI-induced reduction of GABA$_A$R γ_2 intensity (Figure 5A; Table S1; $p_{scr/shRNA}$ = 0.0052) and γ_2 puncta density (Figure S6G; $p_{scr/shRNA}$ = 0.0028) in comparison to cultures with scrambled shRNA controls. Similarly, shRNA knockdown of GPR55 blocked LPI-mediated decreases in gephyrin intensity relative to scrambled shRNA controls (Figure 5A; Table S1; $p_{scr/shRNA}$ = 0.0064) and in gephyrin puncta per unit area (Figure S6G; $p_{scr/shRNA}$ = 0.017). Comparing the effects of CBD and GPR55 shRNA, CBD co-application with LPI (Figure 5A, middle right, red) produced a higher γ_2 level than LPI+shRNA alone (black, $p_{CBD+LPI/LPI-shRNA}$ = 0.017). Together, these observations indicate that LPI decreased the postsynaptic expression of GABA$_A$R γ_2 and gephyrin within 30 min, with reduced puncta density after 60 min. These actions were blocked by CBD and likely mediated by GPR55.

Possible signaling mechanisms linking GPR55 and GABA$_A$R density

A potential control point for LPI effects on GABA$_A$R localization is activity-dependent dephosphorylation of γ_2 serine 327, which increases lateral mobility of GABA$_A$Rs away from gephyrin and destabilizes inhibitory synapses.[40,41] Exposure to LPI gradually reduced phosphorylation of γ_2 S327 in western blots of whole-cell lysates, reaching significance at 30 min (p = 0.0099) and 40 min (p = 0.0033) post LPI (Figure 5B). In contrast, LPI did not significantly alter β_3 S408/409 phosphorylation (Figure S6H), an activity-dependent regulator of GABA$_A$R endocytosis,[42] suggesting that LPI effects on GABA$_A$R might be subunit-specific. Treatment of cultures with 1 μM CBD blocked the LPI-mediated decrease in GABA$_A$R γ_2 S327 dephosphorylation (Figure S6I; p = 0.0027).

We tested a hypothetical mechanism linking GPR55 to γ_2 S327 dephosphorylation. GPR55 is a G_q-linked[24] or $G_{\alpha12/13}$-linked[23,43] GPCR; when signaling via $G_{\alpha13}$, GPR55 communicates to RhoA and Rho-associated protein kinase (ROCK) to discharge internal Ca^{2+} stores.[39] Blockade of ROCK with YM-27632 (10 μM) prevented the LPI-mediated dephosphorylation of γ_2 S327 (Figure 5B; p = 0.76). LPI-induced S327 dephosphorylation remained robust with the blockade of PLC (10 μM U73122, p < 0.0001) or PKC (LPI + 0.1 μM bisindolylmaleimide II p = 0.024). However, LPI γ_2 S327 dephosphorylation was prevented by depleting intracellular Ca^{2+} stores with thapsigargin (10 μM; p = 0.76), inhibition of IP_3Rs with xestospongin C (1 μM; p = 0.41), and calcineurin blockade (10 μM cyclosporine A, p = 0.22), but not PP1α inhibition (5 nM tautomycetin, p = 0.0002). Together, these findings suggest that LPI, communicating via GPR55 and ROCK, signals in a PLC-independent manner to release intracellular Ca^{2+} stores, activate calcineurin, and dephosphorylate GABA$_A$R γ_2 S327, thus dispersing GABA$_A$R clusters (Figure 5B schema).

Seizures elevate GPR55 expression and potentiate pro-excitatory effects of LPI

If LPI-GPR55 signaling shifts the E:I ratio toward hyperexcitability, potentially favoring seizure activity, could seizures reciprocally regulate the LPI-GPR55 axis? To address this, we assessed GPR55 expression ~30 min following acute PTZ-induced seizures. Injection of PTZ in WT mice (105 mg/kg, i.p.) caused a prominent, region-specific elevation in GPR55 immunostaining (Figures 6A and 6B; Table S1), with the highest increases in areas

Please cite this article in press as: Rosenberg et al., Cannabidiol modulates excitatory-inhibitory ratio to counter hippocampal hyperactivity, Neuron (2023), https://doi.org/10.1016/j.neuron.2023.01.018

CellPress
OPEN ACCESS

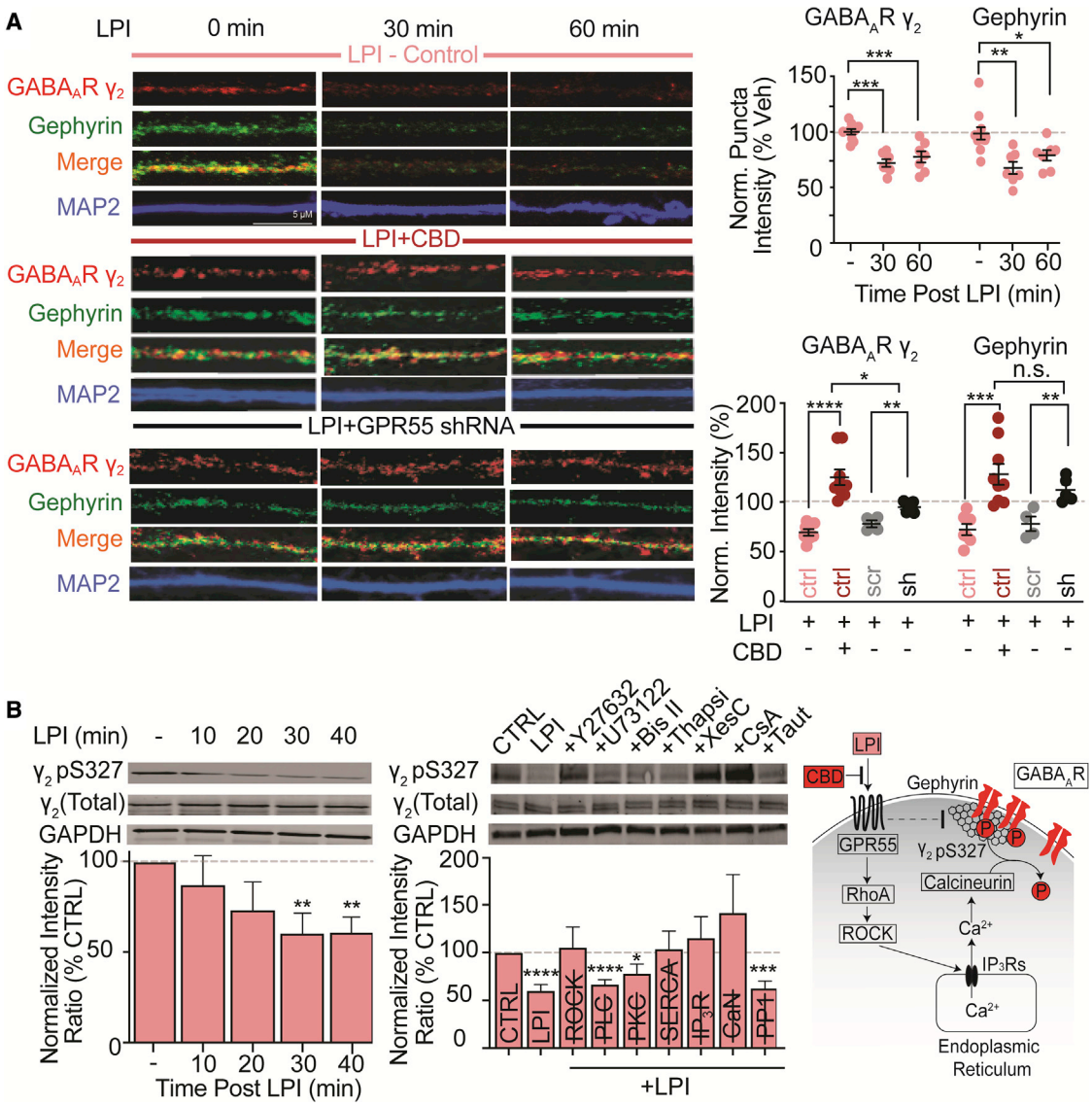

Figure 5. LPI mediates a GPR55-dependent, progressive downregulation of GABA$_A$R γ$_2$ and gephyrin declustering, via S327 dephosphorylation

(A) LPI (4 μM) reduced the intensity of GABA$_A$R γ$_2$ puncta at 30- and 60-min post application (n_{VEH} = 10, $n_{LPI\text{-}30}$ = 7, $n_{VEH/LPI\text{-}60}$ = 7; p_{ANOVA} < 0.0001: $p_{VEH/LPI\text{-}30}$ = 0.0001, $p_{VEH/LPI\text{-}60}$ = 0.0003). LPI also diminished gephyrin puncta intensity at 30- and 60-min post-LPI (p_{ANOVA} = 0.0016: $p_{VEH/LPI\text{-}30}$ = 0.0011, $p_{VEH/LPI\text{-}60}$ = 0.032). CBD (1 μM, red) prevented both LPI-mediated decreases in GABA$_A$R γ$_2$ ($n_{CBD+LPI}$ = 8, $p_{LPI/CBD+LPI}$ < 0.0001) and gephyrin ($p_{LPI/CBD+LPI}$ = 0.0007) puncta at 30 min. Similarly, lentiviral shRNA-mediated knockdown of GPR55 (black, sh, n_{shRNA} = 5) deterred effects of LPI on GABA$_A$R γ$_2$ ($p_{scr/shRNA}$ = 0.0052) and gephyrin (n_{scr} = 5, $p_{scr/shRNA}$ = 0.0064), relative to scrambled shRNA controls (gray, scr, n_{scr} = 5). CBD co-application with LPI produced a higher γ$_2$ level than LPI+shRNA alone ($p_{CBD+LPI/LPI\text{-}shRNA}$ = 0.017).

(B) LPI reduced (γ$_2$ phospho-S327)/(total γ$_2$ expression) in whole hippocampal lysates (n = 8 for all, $p_{LPI\text{-}30}$ = 0.0099; $p_{LPI\text{-}40}$= 0.0033). LPI-mediated S327 dephosphorylation was reversed by inhibitors (n = 4 for all) of RhoA-activated protein kinase (ROCK) (10 μM YM-27632, p = 0.76), IP$_3$Rs (1 μM xestospongin C, p = 0.41), and calcineurin (10 μM cyclosporin, p = 0.22), and by depletion of intracellular calcium stores (10 μM thapsigargin, p = 0.76). However, LPI-mediated effects remained intact in the presence of inhibitors of phospholipase C (10 μM U73122, p < 0.0001), protein kinase C (0.1 μM bisindolylmaleimide II, p = 0.024), and PP1α (5 nm tautomycetin, p = 0.0002). Right, biochemical scheme based on literature[24,39] consistent with pharmacological data.

CA1 (p_{ANOVA} = 0.014: $p_{Non\text{-}Sz+VEH/SZ+VEH}$ = 0.031) and CA3 (p_{ANOVA} = 0.027: $p_{Non\text{-}Sz+VEH/SZ+VEH}$ = 0.044), and a non-significant elevation in DG (p_{ANOVA} = 0.07). *In vivo* pre-treatment with CBD (200 mg/kg, i.p.) 1 h prior to giving PTZ prevented the seizure-induced rise in GPR55 expression (Figures 6A and 6B; Table S1; CA1 $p_{SZ+VEH/Sz+CBD}$ = 0.0069, CA3 $p_{SZ+VEH/Sz+CBD}$ = 0.034). To crosscheck immunostaining data, we probed levels of hippocampal *Gpr55* mRNA by quantitative PCR using newly designed primers demonstrating specificity in KO controls and no associated genomic DNA contamination (Figures S7A and

Please cite this article in press as: Rosenberg et al., Cannabidiol modulates excitatory-inhibitory ratio to counter hippocampal hyperactivity, Neuron (2023), https://doi.org/10.1016/j.neuron.2023.01.018

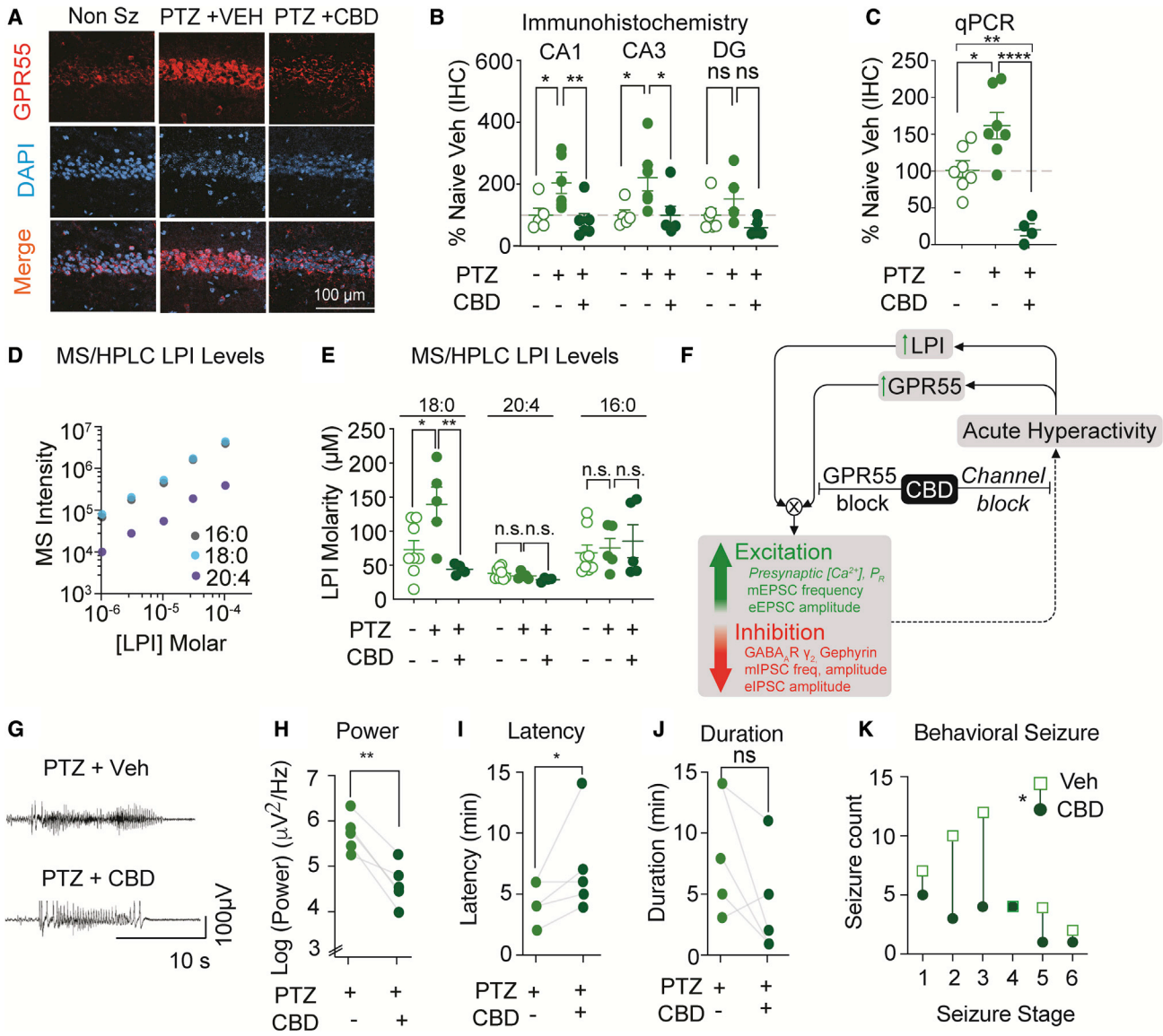

Figure 6. Acute seizures elevate GPR55 expression and increase 18:0 LPI level, effects prevented by CBD pre-treatment

(A and B) Seizures induced by PTZ (105 mg/kg, i.p.) drove region-specific elevations in GPR55 immunoreactivity (n = 6 for all), in areas CA1 (p_{ANOVA} = 0.014, $p_{Non\text{-}Sz+VEH/SZ+VEH}$ = 0.031, representative images) and CA3 (p_{ANOVA} = 0.027, $p_{Non\text{-}Sz+VEH/SZ+VEH}$ = 0.044). The seizure-induced GPR55 elevation was blocked by *in vivo* pre-treatment with CBD (200 mg/kg, i.p.), 1 h prior to giving PTZ (CA1 $p_{SZ+VEH/Sz+CBD}$ = 0.0069, CA3 $p_{SZ+VEH/Sz+CBD}$ = 0.034).

(C) PTZ seizures increase *Gpr55* mRNA expression, prevented by CBD (200 mg/kg, i.p.), 1 h prior to PTZ injection ($n_{Non\text{-}Sz+VEH}$ = 7, n_{Sz+VEH} = 7, n_{Sz+CBD} = 4, p_{ANOVA} < 0.0001, $p_{Non\text{-}Sz+VEH/Sz+VEH}$ = 0.021; $p_{Sz+VEH/SZ+CBD}$ < 0.0001). CBD-treated animals had a lower GPR55 mRNA expression compared with non-seizure, vehicle controls ($p_{Non\text{-}Sz+VEH/Sz+CBD}$ = 0.0060).

(D) Linear standard control curves for 3 LPI isoforms, 16:0, 18:0, 20:4.

(E) PTZ significantly elevated 18:0 LPI, assayed by HPLC-MS ($n_{Non\text{-}Sz+VEH}$ = 8, n_{Sz+VEH} = 5, n_{Sz+CBD} = 4; p_{ANOVA} = 0.0086, $p_{Non\text{-}Sz+VEH/Sz+VEH}$ = 0.031, $p_{Sz+VEH/Sz+CBD}$ = 0.0097).

(F) Simplified depiction of how CBD might oppose acute seizure generation. In proposed scenario, CBD interrupts an acute hyperactivity-induced LPI-GPR55-mediated positive feedback loop. LPI promotes excitability by a dual mechanism: stimulating transient glutamate release and restructuring the inhibitory post-synapse, downregulating inhibition. This elevates the E:I ratio, which likely promotes acute hyperactivity (dotted line) and drives principal cell firing. Hyperactivity in turn upregulates GPR55 and its agonist, LPI. CBD blocks GPR55-dependent pro-excitatory and anti-inhibitory effects of LPI, and also dampens spike firing via direct effects on ion channels[15,16,25–27] thus inhibiting a positive feedback loop that favors hyperactivity. Italics represent findings from prior published studies as indicated above.

(G–K) CBD action on electrographic seizures. Representative EEG traces (G) and quantification demonstrating that CBD (100 mg/kg, i.p.) administered 1 h prior to PTZ (60 mg/kg, i.p.)-induced seizures[44] reduces electrographic seizure average power (H, p = 0.0036), increases latency to first electrographic seizure (I, p = 0.040), and produces a non-significant trend toward reduced EEG seizure duration (J, p = 0.11). (K) CBD decreases behaviorally observed PTZ-induced seizures at Racine stages 1–6 relative to matched vehicle-treated control animals (p = 0.047).

Please cite this article in press as: Rosenberg et al., Cannabidiol modulates excitatory-inhibitory ratio to counter hippocampal hyperactivity, Neuron (2023), https://doi.org/10.1016/j.neuron.2023.01.018

S7B). Assessment of *Gpr55* mRNA by qPCR supported immunostaining data, with a 60% increase in transcripts following PTZ treatment, which were more than fully reversed by CBD pre-treatment (Figure 6C; Table S1; $p_{ANOVA} < 0.0001$: $p_{Non\text{-}Sz+VEH/Sz+VEH} = 0.021$, $p_{Sz+VEH/SZ+CBD} < 0.0001$, $p_{Non\text{-}Sz+VEH/Sz+CBD} = 0.0060$). Thus, ICC and qPCR both showed that seizures elevate GPR55 expression acutely post-seizure induction, with effects blocked by CBD pre-treatment.

To assay LPI levels after seizures, we used liquid chromatography-mass spectrometry targeting LPI isoforms (Figures 6D and 6E; Figures S7C and S7D; Tables S1 and S2). The level of 1-stearoyl LPI (C18:0), the predominant LPI component in brain,[45] was increased 30 min post-PTZ-induced seizure ($p_{ANOVA} = 0.0086$: $p_{Non\text{-}Sz+VEH/Sz+VEH} = 0.031$), an elevation prevented by CBD pre-treatment 1 h prior to PTZ ($p_{Sz+VEH/Sz+CBD} = 0.0097$). Levels of other LPI isoforms (20:4 and 16:0) remained unchanged. Our findings of hyperactivity-induced elevations in GPR55 and its endogenous ligand LPI suggest a positive feedback loop (Figure 6F) that upregulates excitatory and downregulates inhibitory synaptic strength. These synaptic effects could work autocatalytically to promote circuit excitability, producing a vulnerable self-propagating system. By antagonizing LPI activation of GPR55, CBD counteracts LPI's pro-excitability action, lowering GPR55 and LPI levels and dampening the positive feedback. Additionally, CBD could also dampen excitability through a GPR55-independent effect on excitatory ion channels,[25–27] which could restrain activity-dependent GPR55 gene expression and LPI release.[22] We predict that these putative mechanisms operate at different stages to act synergistically, enabling CBD to attenuate electrographic seizure activity.

To assess CBD's role in electrographic seizures, we employed a PTZ model,[44] in a refinement of our earlier protocol (Figures 1C and 1D; Figure S1). We placed electrodes to capture a larger spatial range of electrographic activity in frontal, temporal (hippocampus), and occipital lobes, and used a lower concentration of PTZ (60 mg/kg) as a milder stimulus that would not cause status epilepticus. Pre-treatment with 200 mg/kg CBD decreased average EEG power (Figures 6G and 6H; Figures S7E and S7F; log(power): $p = 0.0036$), increased the latency to first electrographic seizures (Figure 6I, $p = 0.04$), and produced a non-significant trend toward abbreviation of EEG seizure duration ($p = 0.11$). Thus, CBD reduced electrographically recorded seizures, consistent with our hypothesis (Figure 6F). In these animals, CBD also limited behaviorally observed seizures rated over Racine stages 1–6 (Figure 6K, $p = 0.047$).

Enhanced LPI-GPR55 signaling in a model of temporal lobe epilepsy

We next asked whether a seizure-induced rise in GPR55 could potentiate LPI's effect in a chronic model of epilepsy. We used a low mortality, high morbidity model of lithium-pilocarpine (Li-PLC)-induced status epilepticus in male Wistar-Kyoto rats[46] in which CBD given during the epileptogenic period reduced chronic seizure burden[14] (Figure 7A; see STAR Methods). Following status epilepticus, epileptogenesis was determined using a validated post-seizure behavioral battery (PSBB) test; only animals with PSBB scores >10 following a 10-week period were used for experimental study.[46] At 3–6 months after Li-PLC-induced epileptogenesis, there was a non-significant rise in *Gpr55* mRNA (55% ± 29%) relative to non-epileptic age-matched controls (Figure 7B; Table S1; $p_{ANOVA} = 0.19$), with greater experimental variability potentially due to lower *Gpr55* expression in rats vs. mice (Figure S8A; $p_{rat/mice} = 0.0043$). However, GPR55 protein expression, assessed by IHC at 20× resolution, roughly doubled in CA1, CA3, and DG following Li-PLC epileptogenesis (Figure 7C; Table S1; CA1 $p_{ANOVA} = 0.024$: $p_{CTRL/Li\text{-}PLC+VEH} = 0.020$; CA3 $p_{ANOVA} = 0.027$: $p_{CTRL/Li\text{-}PLC+VEH} = 0.028$; DG $p_{ANOVA} = 0.0084$: $p_{CTRL/Li\text{-}PLC+VEH} = 0.014$). CBD 200 mg/kg delivered *p.o.* (*per orem*)) during the weeks following confirmation of epileptogenesis prevented GPR55 elevation in all three areas (Figure 7C; Table S1; CA1 $p_{Li\text{-}PLC+VEH/Li\text{-}PLC+CBD} = 0.042$, CA3 $p_{Li\text{-}PLC+VEH/Li\text{-}PLC+CBD} = 0.042$, DG $p_{Li\text{-}PLC+VEH/Li\text{-}PLC+CBD} = 0.0096$). In CA1 S.R., a locus of synaptic inputs onto CA1 neurons, the normalized intensity of GPR55 colocalized with excitatory nerve terminals marked by VGLUT1 was enhanced ~4-fold following Li-PLC induction (Figure 7D; Table S1; $p_{ANOVA} = 0.0069$: $p_{CTRL/Li\text{-}PLC+VEH} = 0.006$), but not if CBD was given orally following the period of epileptogenesis ($p_{Li\text{-}PLC+VEH/Li\text{-}PLC+CBD} = 0.022$). A similar pattern was seen in S.P. (Figure S8B), where axons originating in area CA3 also course.[47] Li-PLC epileptogenesis induced a 27% ± 8% increase in GPR55 puncta intensity at presumed postsynaptic inhibitory sites labeled with gephyrin in S.P., an effect prevented by chronic *p.o.* CBD (Figure 7E; Table S1; $p_{ANOVA} = p = 0.0007$: $p_{CTRL/Li\text{-}PLC+VEH} = 0.04$, $p_{Li\text{-}PLC+VEH/Li\text{-}PLC+CBD} = 0.0004$). A comparable effect was seen in the S.R. (Figure S8C). The intensity of GPR55 puncta colocalized with VGAT, a presynaptic marker of inhibitory synapses, was nearly doubled following Li-PLC administration (Figures S8D and S8E), effects prevented by CBD, *p.o.* in S.R. (Figure S8D), but not in S.P. (Figure S8E). Simultaneously, major LPI isoform levels (18:0, 20:4, and 16:0) were unchanged following Li-PLC epileptogenesis (Figure S8F; Table S2; 18:0 $p_{ANOVA} = 0.20$; 20:4 $p_{ANOVA} = 0.45$, 16:0 $p_{ANOVA} = 0.76$). In hippocampal tissue, the concentration of 18:0 LPI [LPI] was ~0.1–1 μM in rat, slightly lower than prior reports of [LPI],[45] while roughly 100- to 1,000-fold lower than [LPI] detected in mouse (10–100 μM, Figures 6D and 6E; Table S2). Collectively, Li-PLC-induced epileptogenesis increases GPR55 protein levels, but not the agonist LPI, for several months following induction; increases were prevented by chronic CBD treatment.

The pro-excitatory effects of exogenous LPI in acute slices, taken ~3 months after recurrent seizure induction, were strongly potentiated relative to non-epileptic controls (Figure 7F). The LPI-mediated rise in mEPSC frequency was greater in slices from Li-PLC-treated animals, an increase prevented by chronic *in vivo* treatment with CBD 200 mg/kg given *p.o.* following epileptogenesis (Figure 7F; Table S1; $p_{ANOVA} = 0.0099$: $p_{CTRL/Li\text{-}PLC+VEH} = 0.038$; $p_{Li\text{-}PLC+VEH/Li\text{-}PLC+CBD} = 0.0087$). The potentiation by LPI also persisted for at least 20 min following washout ($p_{ANOVA} = 0.01$: $p_{CTRL/Li\text{-}PLC+VEH}$ $p = 0.012$, $p_{Li\text{-}PLC+VEH/Li\text{-}PLC+CBD}$ $p = 0.034$). The mEPSC amplitude remained unchanged throughout (Figures S8G and S8H, $p_{ANOVA} = 0.26$). LPI produced a greater dis-inhibitory response in mIPSC amplitude in epileptic vs. non-epileptic controls, effects prevented by *in vivo* CBD *p.o.* treatment (Figure 7G; Table S1; $p_{ANOVA} = 0.0032$: $p_{CTRL/Li\text{-}PLC+VEH} = 0.0017$, $p_{Li\text{-}PLC+VEH/Li\text{-}PLC+CBD} = 0.047$), whereas LPI did not diminish mIPSC frequency (Figures S8I and S8J; $p_{ANOVA} = 0.95$). LPI's effects on excitatory and inhibitory currents

Please cite this article in press as: Rosenberg et al., Cannabidiol modulates excitatory-inhibitory ratio to counter hippocampal hyperactivity, Neuron (2023), https://doi.org/10.1016/j.neuron.2023.01.018

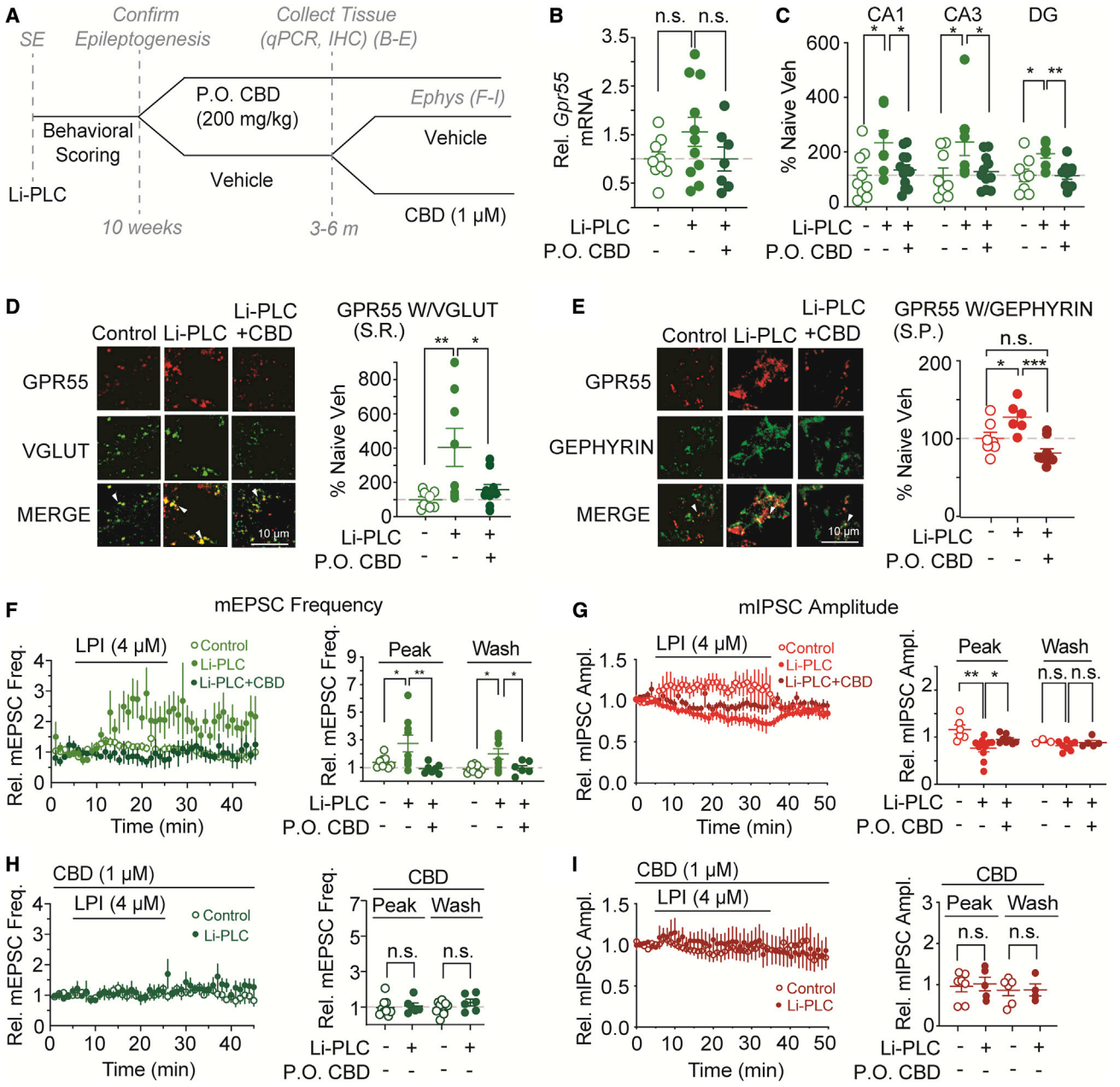

Figure 7. CBD prevents lithium-pilocarpine epileptogenesis-induced elevation of GPR55 immunoreactivity and LPI responsiveness

(A) Experimental paradigm for Li-PLC epileptogenesis (see STAR Methods).[14,46]

(B) Li-PLC epileptogenesis induces a 55% ± 29% elevation in hippocampal *Gpr55* mRNA expression without reaching statistical significance (n_{CTRL} = 9, $n_{Li\text{-}PLC+VEH}$ = 11, $n_{Li\text{-}PLC+CBD}$ = 7, p_{ANOVA} = 0.19).

(C) Li-PLC epileptogenesis increases hippocampal GPR55 immunoreactivity (IHC, 20× resolution), in area CA1 (CA1 n_{CTRL} = 9, $n_{Li\text{-}PLC\text{-}VEH}$ = 7; p_{ANOVA} = 0.024: $p_{CTRL/Li\text{-}PLC+VEH}$ = 0.020), CA3 (n_{CTRL} = 9, $n_{Li\text{-}PLC\text{-}VEH}$ = 8; p_{ANOVA} = 0.027: $p_{CTRL/Li\text{-}PLC+VEH}$ = 0.028), and DG (n_{CTRL} = 8, $n_{Li\text{-}PLC\text{-}VEH}$ = 7; p_{ANOVA} = 0.0084: $p_{CTRL/Li\text{-}PLC+VEH}$ = 0.014). CBD, administered 200 mg/kg *p.o.* after the period of epileptogenesis, prevents the rise in GPR55 expression in CA1 ($n_{Li\text{-}PLC+CBD}$ = 12, $p_{Li\text{-}PLC+VEH/Li\text{-}PLC+CBD}$ = 0.042), CA3 ($n_{Li\text{-}PLC+CBD}$ = 11, $p_{Li\text{-}PLC+VEH/Li\text{-}PLC+CBD}$ = 0.042), and DG ($n_{Li\text{-}PLC+CBD}$ = 10, $p_{Li\text{-}PLC+VEH/Li\text{-}PLC+CBD}$ = 0.0096).

(D) Li-PLC epileptogenesis increases GPR55 puncta intensity colocalized with VGLUT1 at putative presynaptic excitatory terminals in CA1 *stratum radiatum* (S.R., 63×); effect prevented by chronic *p.o.* CBD. Left: representative images, Right: (n_{CTRL} = 8, $n_{Li\text{-}PLC\text{-}VEH}$ = 8, $n_{Li\text{-}PLC+CBD}$ = 10; p_{ANOVA} = 0.0069: $p_{CTRL/Li\text{-}PLC+VEH}$ = 0.006, $p_{Li\text{-}PLC+VEH/Li\text{-}PLC+CBD}$ = 0.022).

(E) GPR55 intensity increases at putative postsynaptic inhibitory sites labeled with gephyrin (S.R., 63×), following Li-PLC-induced epileptogenesis, prevented by CBD treatment after the period of epileptogenesis. Left: representative images, Right: n_{CTRL} = 7, $n_{Li\text{-}PLC\text{-}VEH}$ = 6, $n_{Li\text{-}PLC\text{-}VEH}$ = 9; p_{ANOVA} = 0.0007: $p_{CTRL/Li\text{-}PLC+VEH}$ = 0.04, $p_{Li\text{-}PLC+VEH/Li\text{-}PLC+CBD}$ = 0.0004).

(legend continued on next page)

Please cite this article in press as: Rosenberg et al., Cannabidiol modulates excitatory-inhibitory ratio to counter hippocampal hyperactivity, Neuron (2023), https://doi.org/10.1016/j.neuron.2023.01.018

were blocked by *ex vivo* acute pre-treatment of slices with 1 μM CBD (mEPSCs, Figure 7H, p = 0.76; mIPSCs, Figure 7I: p = 0.77). Together, our data indicate that Li-PLC epileptogenesis increases GPR55 protein expression, potentiates synaptic responses to LPI, and prolongs LPI's effect on mEPSC frequency. All these post-epilepsy changes were abolished by orally delivered CBD (Figures 7F and 7G), in accord with the blocking of the Li-PLC-induced elevation of GPR55 (Figures 7D and 7E), consistent with the posited *in vivo* positive feedback loop (Figure 6F).

CBD prevents "two-pulse" potentiation of KA-induced seizures

To evaluate the contribution of the GP55-LPI axis to seizure susceptibility with more precise temporal control, we examined GPR55 changes 4 and 48 h following injection with kainic acid (KA), a chemoconvulsant model of temporal lobe seizures,[48] (STAR Methods). We chose a two-pulse protocol to determine whether a peri-threshold dose, slightly below that required to consistently elicit seizures, might lead to seizures if repeated days later. We predicted that the first dose ("KA1") might initiate a rise in GPR55, as in the positive feedback proposal (Figure 6F), which could then lower the seizure threshold for an identical KA dose days afterward ("KA2").

Hippocampal *Gpr55* mRNA expression was elevated by 70% at 48 h following the first largely subconvulsive dose of KA (KA1, 24 mg/kg, subcutaneous [s.c.]) (Figure 8A; Table S1; $p_{ANOVA} = 0.018$: $p_{Non\text{-}Sz+Veh/KA1+Veh} = 0.039$). In contrast, no significant change was seen 4 h after KA1 (p = 0.86). Giving CBD (200 mg/kg) 1 h prior to KA1 (CBD1) prevented the rise in GPR55 mRNA at 48 h ($p_{KA1+Veh/KA1+CBD1} = 0.039$). In the same animals used for qPCR, no significant difference appeared in KA1 seizure incidence following administration of CBD1 vs. VEH1 (3/6 animals each, p = 0.11). Consistent with qPCR findings, IHC revealed an increase in GPR55 intensity in hippocampal CA1 and CA3, 48 h post KA1 administration, effects prevented by CBD treatment 1 h prior to KA1 (Figure 8B; Table S1; CA1 $p_{ANOVA} = 0.02$: $p_{Non\text{-}Sz+VEH/KA1+VEH} = 0.040$, $p_{KA1+VEH/KA1+CBD1} = 0.048$; CA3 $p_{ANOVA} < 0.0001$: $p_{Non\text{-}Sz+VEH/KA1+VEH} = 0.0006$, $p_{KA1+VEH/KA1+CBD1} = 0.0001$; DG $p_{ANOVA} = 0.09$).

Consistent with elevated GPR55 expression 2 days after the initial KA challenge, we found that more animals exhibited tonic-clonic seizures after a second KA dose (14/15) than after KA1 (2/15, p < 0.0001; Figure 8C). CBD administration reduced the incidence of second-pulse seizures when given 1 h prior to the second KA2 pulse (CBD2: 1/6, p = 0.0017), potentially due to CBD's acute anti-seizure effect. However, CBD also reduced KA2 seizure incidence when given before the first priming, subconvulsive KA1 dose, 48 h prior to the second KA dose (CBD1: 3/6, p = 0.05). The effect of CBD1 on second-pulse seizures (48 h later) suggests an enduring effect on cellular signaling, not just acute dampening of excitability (Figure 6F) that would readily reverse over the 48 h prior to KA2, given the *in vivo* half-life of CBD injected i.p. (~4–9 h).[29] Collectively, these results support the hypothesis that seizure-induced increases in GPR55 lower the threshold for subsequent seizures (Figure 6F). CBD blockade of increased GPR55 (Figure 8A) provides a potential mechanism for anti-seizure action (Figure 8C), although further study using GPR55 KO mice is warranted in order to confirm correlative findings.

DISCUSSION

CBD restores E:I ratio and disrupts seizure-induced LPI-GPR55-mediated positive feedback loop

Our experiments provide new insights on synaptic mechanisms of CBD's anti-seizure effects. CBD prevented the LPI-driven, GPR55-mediated shift in E:I ratio favoring hyperexcitability. Effects of LPI occurred via two complementary mechanisms: a prompt rise in presynaptic excitatory transmission[22] followed by a gradual and prolonged reduction in postsynaptic inhibitory strength. By blocking both LPI effects, CBD curbed increases in E:I ratio that would drive hippocampal circuits toward hyperexcitability. Further, we discovered that acute PTZ seizures increase GPR55 and LPI expression, and slices from animals with Li-PLC-induced epileptogenesis display exaggerated LPI responsiveness, consistent with potentiated GPR55 activity. We propose a pathogenic positive feedback loop (Figure 6F), hypothesized as E:I regulation gone awry, that provides one of several potential targets for the seizure-reducing effects of CBD (Figures 6, 7, and 8). Our findings complement and extend earlier *in vitro* data demonstrating that CBD (1) blocks LPI-mediated increases in excitatory synaptic weights[22] and (2) upregulates intrinsic firing of PV+ interneurons and spontaneous IPSC frequency.[15,16]

LPI mediates and CBD prevents reduced inhibitory synaptic weight through $GABA_AR$ modulation

LPI reduced inhibitory synaptic weight by dispersing $GABA_AR\ \gamma_2$ and its scaffolding partner gephyrin. LPI's effects at inhibitory synapses were absent in GPR55 KO slices, blocked by CBD, and dependent on intracellular calcium stores, consistent with findings at excitatory synapses. However, unlike GPR55-mediated enhancement of excitatory transmission, which was presynaptically expressed and strikingly transient[22] (Figures 2 and 3), GPR55-dependent downregulation of inhibitory postsynaptic weights developed gradually and lasted 25–30 min post-LPI

(F) Pro-excitatory *ex vivo* effects of the GPR55 agonist LPI were potentiated in slices from rats following Li-PLC-induced epileptogenesis (filled light green circles) in comparison to non-epileptic controls (unfilled light green circles), effects prevented by chronic *in vivo* treatment with CBD *p.o.* (filled dark green circles). Vertical axis, normalized values relative to pre-LPI baseline; mEPSC freq: ($n_{CTRL} = 9$, $n_{Li\text{-}PLC+VEH} = 9$, $n_{Li\text{-}PLC+CBD} = 7$; $p_{ANOVA} = 0.0099$: $p_{CTRL/Li\text{-}PLC+VEH} = 0.038$; $p_{Li\text{-}PLC+VEH/Li\text{-}PLC+CBD} = 0.0087$). The potentiated effects of LPI also persisted following washout ($p_{ANOVA} = 0.01$: $p_{CTRL/Li\text{-}PLC+VEH}$ p = 0.012, $p_{Li\text{-}PLC+VEH/Li\text{-}PLC+CBD}$ p = 0.034).

(G) LPI produced a greater anti-inhibitory drop in mIPSC amplitude in epileptic (filled light red circles) vs. non-epileptic controls (unfilled light red circles), effects prevented by *in vivo* CBD *p.o.* treatment (filled dark red circles, $n_{CTRL} = 6$, $n_{Li\text{-}PLC+VEH} = 10$, $n_{Li\text{-}PLC+CBD} = 8$; $p_{ANOVA} = 0.0032$: $p_{CTRL/Li\text{-}PLC+VEH} = 0.0017$; $p_{Li\text{-}PLC+VEH/Li\text{-}PLC+CBD} = 0.047$).

(H and I) Acute CBD (1 μM) blocked LPI effects on both mEPSC frequency (H) and mIPSC amplitude (I) in both Li-PLC slices and non-epileptic controls.

Please cite this article in press as: Rosenberg et al., Cannabidiol modulates excitatory-inhibitory ratio to counter hippocampal hyperactivity, Neuron (2023), https://doi.org/10.1016/j.neuron.2023.01.018

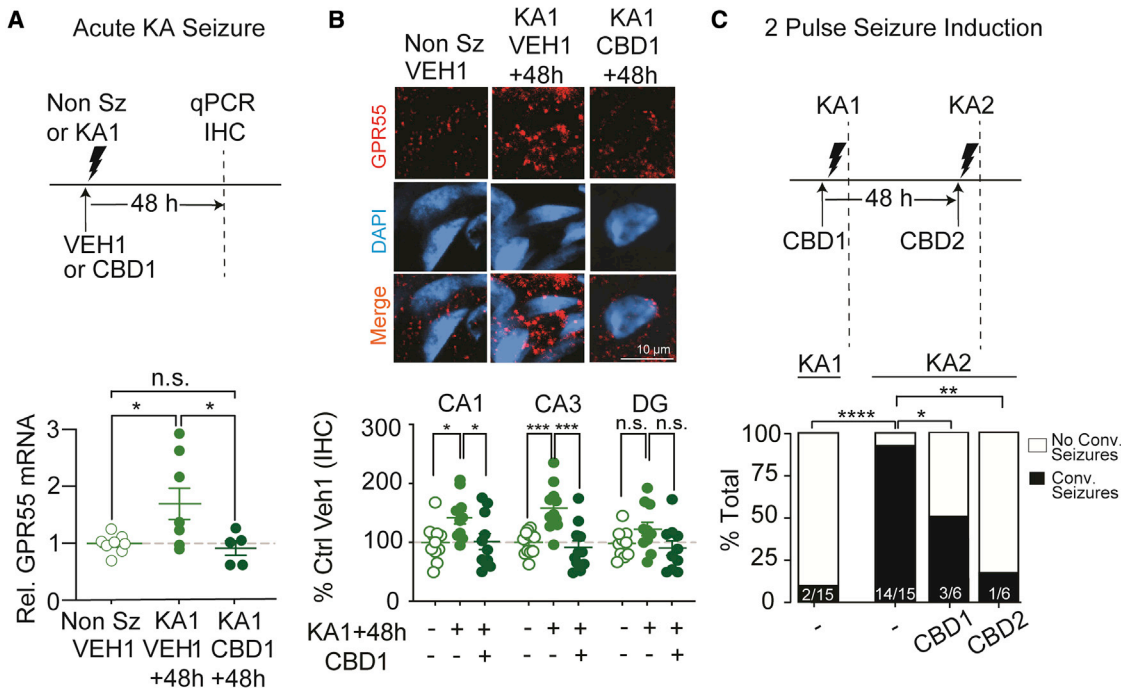

Figure 8. CBD decreases "second-dose" kainic acid (KA)-induced seizures

(A) *Gpr55* mRNA expression was significantly increased 48 h following kainic acid injection (KA1, 24 mg/kg, s.c.) relative to vehicle-treated, non-seizure controls ($n_{Non\text{-}Sz+Veh} = 8$, $n_{KA1+VEH} = 8$; $p_{ANOVA} = 0.018$: $p_{Non\text{-}Sz+Veh/KA1+Veh} = 0.039$). However, pre-treatment with CBD (200 mg/kg, s.c.) 1 h prior to KA1 injection prevented the rise in *Gpr55* mRNA at 48 h ($n_{KA1+CBD1} = 5$, $p_{KA1+Veh/KA1+CBD1} = 0.039$).

(B) GPR55 immunoreactivity increases in CA1 and CA3 48 h post-KA1, effects prevented by CBD 200 mg/kg 1 h prior to KA1 (CA1: n = 11 for all, $p_{ANOVA} = 0.02$: $p_{Non\text{-}Sz+VEH/KA1+VEH} = 0.040$, $p_{KA1+VEH/KA1+CBD1} = 0.048$; CA3: $n_{Non\text{-}Sz+VEH} = 12$, $n_{KA1+VEH} = 11$, $n_{KA1+CBD1} = 11$, $p_{ANOVA} < 0.0001$: $p_{Non\text{-}Sz+VEH/KA1+VEH} = 0.0006$, $p_{KA1+VEH/KA1+CBD1} = 0.0001$; DG: $n_{Non\text{-}Sz+VEH} = 11$, $n_{KA1+VEH} = 11$, $n_{KA1+CBD1} = 10$, $p_{ANOVA} = 0.09$).

(C) Effects of 2nd dose of KA administered 48 h post KA1 (KA2, 24 mg/kg, s.c.). Behavioral seizures assessed via modified Racine scale, 2 h after KA1 or KA2 (timing of assays, dashed vertical lines), followed by injection with diazepam 10 mg/kg, s.c. Although 2/15 animals demonstrated convulsive seizures (as defined as 3–4 on Racine scale) following KA1, a significantly greater proportion displayed KA-induced seizures after KA2 (14/15, $p < 0.0001$, Fisher's exact test). CBD (200 mg/kg, s.c.) reduced the frequency of convulsive seizures following KA2 when CBD was administered 1 h prior to KA1 injection (CBD1, $p = 0.05$) or 1 h prior to KA2 (CBD2, $p = 0.0017$). There was no significant difference between KA1 seizure incidence with CBD1 or VEH1 administration ($p = 0.11$, data not shown).

application. LPI reduced $GABA_AR$ phosphorylation at γ_2 S327, a phosphorylation site regulating γ_2 subunit lateral movement from gephyrin to extrasynaptic sites,[37,40,41] corresponding to a slow, progressive decreases in mIPSC amplitude and frequency. Our data align with findings demonstrating several forms of inhibitory synapse plasticity via γ_2 dephosphorylation.[40,49,50] We found that S327 dephosphorylation depended on IP_3R-mediated calcium release, calcineurin, and RhoA/ROCK kinase,[40,41] but not phospholipase C (Figure 5B).[43] We predict that LPI might activate IP_3Rs directly,[51] bypassing PLC-mediated IP_3 formation, to drive Ca^{2+} release and CaN activation, prompting future biochemical studies. Beyond effects on γ_2, LPI reduced the intensity and number of gephyrin puncta, which regulates synaptic localization of $GABA_AR$ γ_2-containing heteromers.[52,53] Immunolabeled puncta of γ_2 and gephyrin diminished together, as if LPI-induced changes in γ_2 and gephyrin operate coordinately to disperse inhibitory complexes and decrease mIPSC frequency, inhibitory weights, and IPSC amplitude. In *ex vivo* hippocampal slices, GPR55 puncta were found in the pyramidal cell layer, representing presumptive gephyrin-labeled inhibitory synapses, although effects on excitability, cell structure, cell-cell interactions, or excitatory synapses, given colocalization with PSD-95, are also possible (Figure S3).

LPI acts in partial opposition to E:I modulatory actions of eCBs and LPA, and undergoes activity-dependent release

By elevating presynaptic glutamate release and reducing inhibitory synaptic strength, LPI shifts the E:I ratio toward hyperexcitability, providing a powerful transient signal amplifier. This contrasts with the stabilizing "circuit breaker" function of eCBs, which counteracts excess network activity by reducing both excitatory and inhibitory presynaptic release.[6,33,54,55] Similarly, lysophosphatidic acid (LPA), a bioactive lipid related to LPI, stabilizes synaptic circuits by depressing presynaptic excitatory release and reducing inhibitory tone by disaggregating postsynaptic $GABA_AR$.[41] Thus, while eCBs and LPA generally weaken excitation and inhibition together, LPI reduces postsynaptic inhibitory weights while elevating glutamate release. LPI's actions strongly increase the E:I ratio, enabling LPI to powerfully amplify incoming signals following activity-dependent stimulation. We propose that eCBs, LPI, and LPA serve as strategic

Please cite this article in press as: Rosenberg et al., Cannabidiol modulates excitatory-inhibitory ratio to counter hippocampal hyperactivity, Neuron (2023), https://doi.org/10.1016/j.neuron.2023.01.018

control points for the modulation of brain excitability, as these lipid modulators are enzymatically interconnected.[7]

Acute PTZ-induced hyperexcitability increased levels of the major LPI isoform (18:0),[45] consistent with multiple evidentiary lines for activity-dependent enhancement of LPI generation and release. First, LPI synthesis partially depends on secretory phospholipase A2 (PLA2),[7] a Ca^{2+}-dependent enzyme[56] whose levels are elevated by seizures.[57] Second, PLA2-driven LPI synthesis/release is likely elevated by bursts of presynaptic firing, reflected by effects of CBD and inhibitors of PLA2.[22] Third, CBD efficacy increases with graded neuronal depolarization, consistent with depolarization-induced LPI release.[16] These data suggest that stimulus-driven, phasic release of LPI provides a short-lasting signal that in moderation enhances information transfer and circuit function. However, following seizure-induced elevations, GPR55's neuromodulatory control could lead to the proposed pathological positive feedback (Figure 6F), magnifying and prolonging LPI's pro-excitatory effect (Figure 7F). Genetic evidence supports the pathological potential of LPI: epilepsy and intellectual disability arise from inactivating mutations in LPI acyltransferase, the enzyme that converts LPI to its PI precursor.[58]

Elevated LPI-GPR55 signaling is a target of CBD's anti-seizure action

To evaluate GPR55 as a potential target for CBD's anti-seizure actions, we assessed multiple rodent models of acute seizures and chronic epileptogenesis, each with advantages and drawbacks. As acute seizure models, we used proconvulsants PTZ (a $GABA_AR$ antagonist to model disinhibition; Figures 1 and 6) and KA (a GluR agonist) to model temporal lobe seizures (Figure 8). Acute PTZ seizure induction upregulated GPR55 at both mRNA and protein levels, 30 min following PTZ injection (Figures 6B and 6C), and acutely elevated the 18:0 isoform of LPI (Figure 6E). Further, *Gpr55* mRNA increased 48 h following a single dose of KA, consistent with elevated "second-pulse" seizure susceptibility (Figure 8). Seizure-induced increases in GPR55 expression were prevented by CBD pre-treatment at doses that yielded anti-seizure effects *in vivo* (200 mg/kg, Figure 1C). A relatively higher dose of CBD was selected due to multiple factors including pharmacokinetics following acute delivery, rapid distribution of lipid soluble CBD into hydrophobic tissue, and a species difference brain:plasma concentration ratio in mice relative to other species (see Epidyolex EMA Assessment 2019).[29]

CBD's anticonvulsive effects on PTZ-induced seizures were absent in GPR55 KO mice (Figure 1C), consistent with GPR55's role in seizure generation and CBD antagonism of GPR55 (Figure 6F). A potential confound is that PTZ-induced seizures were more prevalent in GPR55 KO mice than would be expected in comparison to peak CBD suppression in WT animals (Figure 1C). This difference might arise from GPR55's absence during development, when LPI-GPR55 signaling contributes to axon pathfinding and synapse maturation.[30,59] Hints of possible compensatory effects were evident in unitary excitatory synaptic weights, which were greater in GPR55 KO than WT slices (Figure S2A). To address this potential confound, future studies could examine conditional deletion of GPR55 later in development.

We also studied spontaneously recurrent seizures using Li-PLC induction in rats and found that GPR55 protein expression was persistently elevated several months following the epileptogenic insult (Figure 7C). GPR55 protein levels in hippocampal regions doubled relative to age-matched controls, but not if CBD was given orally during the epileptogenic period at doses that reduce chronic seizure burden.[14] Epileptogenesis triggered a non-significant, variable increase in *Gpr55* mRNA compared with acute PTZ-treated mice (Figure 6B), potentially due to lower *Gpr55* mRNA in rat vs. mice (Figure S8A) or differences in seizure model. A rise in GPR55 protein (IHC), but not mRNA, could be attributable to post-transcriptional changes in GPR55, including activity-dependent alterations in endocytosis and surface expression as previously reported with CB_1Rs,[60] or obscuring of region-specific changes in whole hippocampal qPCR. Consistent with GPR55 elevation at excitatory and inhibitory synaptic loci (Figures 7D and 7E; Figures S8B–S8E), corresponding synaptic responses to exogenous LPI were strikingly enhanced (Figures 7F and 7G), but absent with CBD. We applied CBD at 1 μM, sufficient to antagonize GPR55 (IC_{50} 445 ± 67 nM),[23] in line with peak plasma levels (>1 μM) in Dravet syndrome patients receiving CBD long term (20 mg/kg × 21 days).[61] In the rat Li-PLC model, animals are euthanized several months following the initial epileptic insult, agnostic to the last acute seizure; transient activity-dependent changes in acute LPI release might elude detection. Indeed, levels of LPI assessed in the hippocampus of epileptic rats were not significantly different than non-epileptic controls (Figure S8F). The lack of detectable change in LPI could be due to experimental limitations of lipid isolation or inability to capture fleeting post-seizure changes in LPI, possibly paralleling transient (<∼1 h) seizure-induced elevation in eCBs.[62–64] Future studies could determine whether exogenous LPI suffices to lower threshold for recurrent seizures.

We tentatively propose that CBD can extinguish a potentially regenerative loop in which hyperactivity enhances LPI-GPR55 signaling, further shifting the E:I ratio (Figure 6F). Our conceptual framework incorporates additional non-GPR55-dependent actions, such as a role for CBD reducing excitability via direct effects on ion channels,[25–27] and direct effects of CBD on the synthetic enzyme that produces LPI, PLA2.[65,66] Non-GPR55 targets might explain why CBD reduced seizure-induced mortality in both WT and GPR55 KO mice (Figure 1D) and exerted effects on $GABA_ARs$ above that of GPR55 knockdown alone (Figure 5A), as if CBD also acted directly on $GABA_ARs$.[67] Further candidates for CBD's anti-seizure effects[17,18] include transient receptor potential (TRP) channel (TRPV1, TRPV2, and TRPA1) agonism,[68–71] CB_1R negative allosteric modulation,[19,20] as well as inhibition of ENT-1 adenosine transporter,[72] CaV3.3 channels,[73] mitochondrial VDAC1 channels,[74] and regulation of non-neuronal cells (e.g., glia). In addition, GPR55 could also play a non-synaptic role in regulating ion channel conductances in interneurons,[16] especially PV+ interneurons[15,16,75] through effects of Na_V channels. We propose that CBD might act on non-GPR55 targets to regulate network excitability, opposing potential stimuli that "engage" the hyperactivity-induced feedback loop as described in Figure 6F. However, effects on such non-GPR55 targets that rely on the immediate presence of CBD are unlikely to explain

partial efficacy against KA seizures that persisted 48 h after CBD administration (Figure 8C), long after brain levels declined. Further evaluation of these candidate targets at clinically relevant CBD doses is needed.

A mechanism for CBD synergy with $GABA_AR$ modulation

CBD provides a potential therapeutic agent in treatment-resistant epilepsy patients who did not respond to $GABA_AR$ modulators (e.g., benzodiazepines),[76] possibly due to LPI-GPR55 effects. Our evidence suggests that hyperactivity could trigger LPI-driven synaptic disinhibition, further lowering the threshold for recurrent seizures. $GABA_AR$ γ_2, the target of GPR55 action, has previously been implicated in multiple prior models of seizures. Surface γ_2 levels are decreased in preclinical models of Li-PLC-induced status epilepticus,[77] patients with temporal lobe epilepsy,[78] and pediatric epilepsy with febrile seizures.[79–81] Thus, LPI-mediated reduction in γ_2 and gephyrin levels may be proconvulsive, phenocopying γ_2 mutations causing epilepsy, reducing GABAergic synaptic strength, and further limiting benzodiazepines' full impact. By restoring $GABA_AR$ cluster abundance, CBD might reestablish benzodiazepine efficacy, thus contributing to CBD's clinical efficacy in combination therapy with benzodiazepines,[82,83] beyond possible pharmacokinetic interactions on drug metabolism.[84,85]

STAR★METHODS

Detailed methods are provided in the online version of this paper and include the following:

SUPPLEMENTAL INFORMATION

Supplemental information can be found online at https://doi.org/10.1016/j.neuron.2023.01.018.

ACKNOWLEDGMENTS

We thank Ken Mackie for generously providing the GPR55 KO (*B6;129S-Gpr55^{tm1Lex}/Mmnc*) mice. We gratefully acknowledge GW Research Ltd, Cambridge, UK, for furnishing the CBD (Epidiolex®) used in the study. We thank Pablo Castillo, Jayeeta Basu, and Niels Ringstad for valuable comments on an early draft of this manuscript. Additional analysis code was generously provided by Benjamin Suutari, Natasha Tirko, and Katherine Eyring. We thank the NYU Metabolomics Core and Experimental Pathology Research Laboratory Core (both supported by the Cancer Center Support Grant P30CA016087 at NYU Langone's Laura and Isaac Perlmutter Cancer Center) for their help in acquiring and analyzing the data presented in this report. This work is supported by funding from the Ruth L. Kirschstein National Research Service Awards (NRSA) for individual pre-doctoral MD/PhDs (F30 NS100293), the NYU MSTP training grant (T32GM007308), and grants to R.W.T. from the NIMH (5R37MH071739), NIDA (DA040484-01), the Simons Foundation, and the Vulnerable Brain Project. S.C., A.S., and O.D. are supported by funding from FACES, Finding A Cure for Epilepsy and Seizures. S.C. is supported by a Charles H. Revson Senior Fellowship in Biomedical Science, Andrew Ellis and Emily Segal Investigator Grant from the Brain and Behavior Research Foundation, postdoctoral fellowship from the Fonds de Recherche du Québec - Santé, and a K99/R00 Pathway to Independence Award from NIMH (1K99MH126157-01).

AUTHOR CONTRIBUTIONS

E.C.R., S.C., M.B., B.J.W., H.E.S., and R.W.T. designed the research. E.C.R., S.C., M.B., E.R.N., X.W., S.M., S.J., S.G., M.W., N.M., A.S., S.B., P.H.P., and R.R. performed experiments and analyzed results. N.C. provided imaging analysis code. S.D.S. provided assistance with figure construction. E.C.R. and R.W.T. wrote the paper with contributions from S.C., M.B., D.J., G.B., O.D., G.W., H.E.S., and B.J.W.

DECLARATION OF INTERESTS

GW Research Ltd (Cambridge, UK) supplied plant-derived highly purified CBD to R.W.T., M.B., B.J.W., and G.W. for experimental use and provided funding for animal maintenance for G.W. B.J.W. is an employee of GW Research Ltd, now part of Jazz Pharmaceuticals Inc., Cambridge, UK. M.B. was formerly an employee of GW Research Ltd, now part of Jazz Pharmaceuticals Inc., Cambridge, UK. O.D. receives grant support from NINDS, NIMH, MURI, CDC, and NSF. He has equity and/or compensation from the following companies: Privateer Holdings, Tilray, Receptor Life Sciences, Qstate Biosciences, Tevard, Empatica, Engage, Egg Rock/Papa & Barkley, Rettco, SilverSpike, and California Cannabis Enterprises (CCE). He has received consulting fees from GW Research Ltd, Cavion, and Zogenix. He holds patents for the use of CBD in treating neurological disorders, but these are owned by GW Research Ltd, and he has waived any financial stake in these patents.

INCLUSION AND DIVERSITY

We support inclusive, diverse, and equitable conduct of research.

Received: August 12, 2020
Revised: September 27, 2022
Accepted: January 20, 2023
Published: February 13, 2023

REFERENCES

1. Liu, G. (2004). Local structural balance and functional interaction of excitatory and inhibitory synapses in hippocampal dendrites. Nat. Neurosci. *7*, 373–379. https://doi.org/10.1038/nn1206.
2. Xue, M., Atallah, B.V., and Scanziani, M. (2014). Equalizing excitation-inhibition ratios across visual cortical neurons. Nature *511*, 596–600. https://doi.org/10.1038/nature13321.
3. Paz, J.T., and Huguenard, J.R. (2015). Microcircuits and their interactions in epilepsy: is the focus out of focus? Nat. Neurosci. *18*, 351–359. https://doi.org/10.1038/nn.3950.
4. Rubenstein, J.L., and Merzenich, M.M. (2003). Model of autism: increased ratio of excitation/inhibition in key neural systems. Genes Brain Behav. *2*, 255–267.
5. Lewis, D.A., Curley, A.A., Glausier, J.R., and Volk, D.W. (2012). Cortical parvalbumin interneurons and cognitive dysfunction in schizophrenia. Trends Neurosci. *35*, 57–67. https://doi.org/10.1016/j.tins.2011.10.004.
6. Katona, I., and Freund, T.F. (2008). Endocannabinoid signaling as a synaptic circuit breaker in neurological disease. Nat. Med. *14*, 923–930. https://doi.org/10.1038/nm.f.1869.
7. Yamashita, A., Oka, S., Tanikawa, T., Hayashi, Y., Nemoto-Sasaki, Y., and Sugiura, T. (2013). The actions and metabolism of lysophosphatidylinositol, an endogenous agonist for GPR55. Prostaglandins Other Lipid Mediat. *107*, 103–116. https://doi.org/10.1016/j.prostaglandins.2013.05.004.
8. Rosenberg, E.C., Patra, P.H., and Whalley, B.J. (2017). Therapeutic effects of cannabinoids in animal models of seizures, epilepsy, epileptogenesis, and epilepsy-related neuroprotection. Epilepsy Behav. *70*, 319–327. https://doi.org/10.1016/j.yebeh.2016.11.006.
9. Devinsky, O., Cross, J.H., Laux, L., Marsh, E., Miller, I., Nabbout, R., Scheffer, I.E., Thiele, E.A., and Wright, S.; Cannabidiol in Dravet Syndrome Study Group (2017). Trial of cannabidiol for drug-resistant seizures in the Dravet syndrome. N. Engl. J. Med. *376*, 2011–2020. https://doi.org/10.1056/NEJMoa1611618.
10. Scheffer, I.E., Halford, J.J., Miller, I., Nabbout, R., Sanchez-Carpintero, R., Shiloh-Malawsky, Y., Wong, M., Zolnowska, M., Checketts, D., Dunayevich, E., and Devinsky, O. (2021). Add-on cannabidiol in patients with Dravet syndrome: results of a long-term open-label extension trial. Epilepsia *62*, 2505–2517. https://doi.org/10.1111/epi.17036.
11. Miller, I., Scheffer, I.E., Gunning, B., Sanchez-Carpintero, R., Gil-Nagel, A., Perry, M.S., Saneto, R.P., Checketts, D., Dunayevich, E., Knappertz, V., and Group, G.S. (2020). Dose-ranging effect of adjunctive oral cannabidiol vs placebo on convulsive seizure frequency in Dravet syndrome: A randomized clinical trial. JAMA Neurol. *77*, 613–621. https://doi.org/10.1001/jamaneurol.2020.0073.
12. Devinsky, O., Patel, A.D., Cross, J.H., Villanueva, V., Wirrell, E.C., Privitera, M., Greenwood, S.M., Roberts, C., Checketts, D., VanLandingham, K.E., et al. (2018). Effect of cannabidiol on drop seizures in the Lennox-Gastaut syndrome. N. Engl. J. Med. *378*, 1888–1897. https://doi.org/10.1056/NEJMoa1714631.
13. Thiele, E.A., Bebin, E.M., Bhathal, H., Jansen, F.E., Kotulska, K., Lawson, J.A., O'Callaghan, F.J., Wong, M., Sahebkar, F., Checketts, D., et al. (2021). Add-on cannabidiol treatment for drug-resistant seizures in tuberous sclerosis complex: A placebo-controlled randomized clinical trial. JAMA Neurol. *78*, 285–292. https://doi.org/10.1001/jamaneurol.2020.4607.
14. Patra, P.H., Barker-Haliski, M., White, H.S., Whalley, B.J., Glyn, S., Sandhu, H., Jones, N., Bazelot, M., Williams, C.M., and McNeish, A.J. (2019). Cannabidiol reduces seizures and associated behavioral comorbidities in a range of animal seizure and epilepsy models. Epilepsia *60*, 303–314. https://doi.org/10.1111/epi.14629.
15. Kaplan, J.S., Stella, N., Catterall, W.A., and Westenbroek, R.E. (2017). Cannabidiol attenuates seizures and social deficits in a mouse model of Dravet syndrome. Proc. Natl. Acad. Sci. USA *114*, 11229–11234. https://doi.org/10.1073/pnas.1711351114.
16. Khan, A.A., Shekh-Ahmad, T., Khalil, A., Walker, M.C., and Ali, A.B. (2018). Cannabidiol exerts antiepileptic effects by restoring hippocampal interneuron functions in a temporal lobe epilepsy model. Br. J. Pharmacol. *175*, 2097–2115. https://doi.org/10.1111/bph.14202.
17. Gray, R.A., and Whalley, B.J. (2020). The proposed mechanisms of action of CBD in epilepsy. Epileptic Disord. *22*, 10–15. https://doi.org/10.1684/epd.2020.1135.
18. Ibeas Bih, C., Chen, T., Nunn, A.V., Bazelot, M., Dallas, M., and Whalley, B.J. (2015). Molecular targets of cannabidiol in neurological disorders. Neurotherapeutics J. Am. Soc. Exp. Neurotherapeutics *12*, 699–730. https://doi.org/10.1007/s13311-015-0377-3.
19. Laprairie, R.B., Bagher, A.M., Kelly, M.E., and Denovan-Wright, E.M. (2015). Cannabidiol is a negative allosteric modulator of the cannabinoid CB1 receptor. Br. J. Pharmacol. *172*, 4790–4805. https://doi.org/10.1111/bph.13250.
20. Straiker, A., Dvorakova, M., Zimmowitch, A., and Mackie, K. (2018). Cannabidiol inhibits endocannabinoid signaling in autaptic hippocampal neurons. Mol. Pharmacol. *94*, 743–748. https://doi.org/10.1124/mol.118.111864.
21. Oka, S., Nakajima, K., Yamashita, A., Kishimoto, S., and Sugiura, T. (2007). Identification of GPR55 as a lysophosphatidylinositol receptor. Biochem. Biophys. Res. Commun. *362*, 928–934. https://doi.org/10.1016/j.bbrc.2007.08.078.
22. Sylantyev, S., Jensen, T.P., Ross, R.A., and Rusakov, D.A. (2013). Cannabinoid- and lysophosphatidylinositol-sensitive receptor GPR55 boosts neurotransmitter release at central synapses. Proc. Natl. Acad. Sci. USA *110*, 5193–5198. https://doi.org/10.1073/pnas.1211204110.
23. Ryberg, E., Larsson, N., Sjögren, S., Hjorth, S., Hermansson, N.O., Leonova, J., Elebring, T., Nilsson, K., Drmota, T., and Greasley, P.J. (2007). The orphan receptor GPR55 is a novel cannabinoid receptor. Br. J. Pharmacol. *152*, 1092–1101. https://doi.org/10.1038/sj.bjp.0707460.
24. Lauckner, J.E., Jensen, J.B., Chen, H.Y., Lu, H.C., Hille, B., and Mackie, K. (2008). GPR55 is a cannabinoid receptor that increases intracellular calcium and inhibits M current. Proc. Natl. Acad. Sci. USA *105*, 2699–2704. https://doi.org/10.1073/pnas.0711278105.
25. Zhang, H.B., and Bean, B.P. (2021). Cannabidiol inhibition of murine primary nociceptors: tight binding to slow inactivated states of Nav1.8 channels. J. Neurosci. *41*, 6371–6387. https://doi.org/10.1523/JNEUROSCI.3216-20.2021.
26. Ghovanloo, M.R., Shuart, N.G., Mezeyova, J., Dean, R.A., Ruben, P.C., and Goodchild, S.J. (2018). Inhibitory effects of cannabidiol on voltage-dependent sodium currents. J. Biol. Chem. *293*, 16546–16558. https://doi.org/10.1074/jbc.RA118.004929.
27. Patel, R.R., Barbosa, C., Brustovetsky, T., Brustovetsky, N., and Cummins, T.R. (2016). Aberrant epilepsy-associated mutant Nav1.6 sodium channel activity can be targeted with cannabidiol. Brain *139*, 2164–2181. https://doi.org/10.1093/brain/aww129.
28. Alexander, A., Maroso, M., and Soltesz, I. (2016). Organization and control of epileptic circuits in temporal lobe epilepsy. Prog. Brain Res. *226*, 127–154. https://doi.org/10.1016/bs.pbr.2016.04.007.
29. Deiana, S., Watanabe, A., Yamasaki, Y., Amada, N., Arthur, M., Fleming, S., Woodcock, H., Dorward, P., Pigliacampo, B., Close, S., et al. (2012). Plasma and brain pharmacokinetic profile of cannabidiol (CBD), cannabidivarine (CBDV), Delta(9)-tetrahydrocannabivarin (THCV) and cannabigerol (CBG) in rats and mice following oral and intraperitoneal administration and CBD action on obsessive-compulsive behaviour. Psychopharmacology *219*, 859–873. https://doi.org/10.1007/s00213-011-2415-0.
30. Cherif, H., Argaw, A., Cécyre, B., Bouchard, A., Gagnon, J., Javadi, P., Desgent, S., Mackie, K., and Bouchard, J.F. (2015). Role of GPR55 during axon growth and target innervation. eNeuro *2*. ENEURO.0011-15.2015. https://doi.org/10.1523/ENEURO.0011-15.2015.
31. Kargl, J., Balenga, N., Parzmair, G.P., Brown, A.J., Heinemann, A., and Waldhoer, M. (2012). The cannabinoid receptor CB1 modulates the

signaling properties of the lysophosphatidylinositol receptor GPR55. J. Biol. Chem. *287*, 44234–44248. https://doi.org/10.1074/jbc.M112.364109.

32. Dudok, B., Barna, L., Ledri, M., Szabó, S.I., Szabadits, E., Pintér, B., Woodhams, S.G., Henstridge, C.M., Balla, G.Y., Nyilas, R., et al. (2015). Cell-specific STORM super-resolution imaging reveals nanoscale organization of cannabinoid signaling. Nat. Neurosci. *18*, 75–86. https://doi.org/10.1038/nn.3892.

33. Castillo, P.E., Younts, T.J., Chávez, A.E., and Hashimotodani, Y. (2012). Endocannabinoid signaling and synaptic function. Neuron *76*, 70–81. https://doi.org/10.1016/j.neuron.2012.09.020.

34. Hurst, K., Badgley, C., Ellsworth, T., Bell, S., Friend, L., Prince, B., Welch, J., Cowan, Z., Williamson, R., Lyon, C., et al. (2017). A putative lysophosphatidylinositol receptor GPR55 modulates hippocampal synaptic plasticity. Hippocampus *27*, 985–998. https://doi.org/10.1002/hipo.22747.

35. Pouille, F., and Scanziani, M. (2001). Enforcement of temporal fidelity in pyramidal cells by somatic feed-forward inhibition. Science *293*, 1159–1163. https://doi.org/10.1126/science.1060342.

36. Hu, H., Gan, J., and Jonas, P. (2014). Interneurons. Fast-spiking, parvalbumin(+) GABAergic interneurons: from cellular design to microcircuit function. Science *345*, 1255263. https://doi.org/10.1126/science.1255263.

37. Jacob, T.C., Bogdanov, Y.D., Magnus, C., Saliba, R.S., Kittler, J.T., Haydon, P.G., and Moss, S.J. (2005). Gephyrin regulates the cell surface dynamics of synaptic GABAA receptors. J. Neurosci. *25*, 10469–10478. https://doi.org/10.1523/JNEUROSCI.2267-05.2005.

38. Jacob, T.C., Moss, S.J., and Jurd, R. (2008). GABA(A) receptor trafficking and its role in the dynamic modulation of neuronal inhibition. Nat. Rev. Neurosci. *9*, 331–343. https://doi.org/10.1038/nrn2370.

39. Ross, R.A. (2009). The enigmatic pharmacology of GPR55. Trends Pharmacol. Sci. *30*, 156–163. https://doi.org/10.1016/j.tips.2008.12.004.

40. Muir, J., Arancibia-Carcamo, I.L., MacAskill, A.F., Smith, K.R., Griffin, L.D., and Kittler, J.T. (2010). NMDA receptors regulate GABAA receptor lateral mobility and clustering at inhibitory synapses through serine 327 on the gamma2 subunit. Proc. Natl. Acad. Sci. USA *107*, 16679–16684. https://doi.org/10.1073/pnas.1000589107.

41. García-Morales, V., Montero, F., González-Forero, D., Rodríguez-Bey, G., Gómez-Pérez, L., Medialdea-Wandossell, M.J., Domínguez-Vías, G., García-Verdugo, J.M., and Moreno-López, B. (2015). Membrane-derived phospholipids control synaptic neurotransmission and plasticity. PLoS Biol. *13*, e1002153. https://doi.org/10.1371/journal.pbio.1002153.

42. Kittler, J.T., Chen, G., Honing, S., Bogdanov, Y., McAinsh, K., Arancibia-Carcamo, I.L., Jovanovic, J.N., Pangalos, M.N., Haucke, V., Yan, Z., and Moss, S.J. (2005). Phospho-dependent binding of the clathrin AP2 adaptor complex to GABAA receptors regulates the efficacy of inhibitory synaptic transmission. Proc. Natl. Acad. Sci. USA *102*, 14871–14876. https://doi.org/10.1073/pnas.0506653102.

43. Henstridge, C.M., Balenga, N.A., Ford, L.A., Ross, R.A., Waldhoer, M., and Irving, A.J. (2009). The GPR55 ligand L-alpha-lysophosphatidylinositol promotes RhoA-dependent Ca2+ signaling and NFAT activation. FASEB J. *23*, 183–193. https://doi.org/10.1096/fj.08-108670.

44. Vilela, L.R., Lima, I.V., Kunsch, É.B., Pinto, H.P.P., de Miranda, A.S., Vieira, É.L.M., de Oliveira, A.C.P., Moraes, M.F.D., Teixeira, A.L., and Moreira, F.A. (2017). Anticonvulsant effect of cannabidiol in the pentylenetetrazole model: pharmacological mechanisms, electroencephalographic profile, and brain cytokine levels. Epilepsy Behav. *75*, 29–35. https://doi.org/10.1016/j.yebeh.2017.07.014.

45. Oka, S., Toshida, T., Maruyama, K., Nakajima, K., Yamashita, A., and Sugiura, T. (2009). 2-arachidonoyl-sn-glycero-3-phosphoinositol: a possible natural ligand for GPR55. J. Biochem. *145*, 13–20. https://doi.org/10.1093/jb/mvn136.

46. Modebadze, T., Morgan, N.H., Pérès, I.A., Hadid, R.D., Amada, N., Hill, C., Williams, C., Stanford, I.M., Morris, C.M., Jones, R.S., et al. (2016). A low mortality, high morbidity reduced intensity status epilepticus (RISE) model of epilepsy and epileptogenesis in the rat. PLoS One *11*, e0147265. https://doi.org/10.1371/journal.pone.0147265.

47. Ropireddy, D., Scorcioni, R., Lasher, B., Buzsáki, G., and Ascoli, G.A. (2011). Axonal morphometry of hippocampal pyramidal neurons semi-automatically reconstructed after in vivo labeling in different CA3 locations. Brain Struct. Funct. *216*, 1–15. https://doi.org/10.1007/s00429-010-0291-8.

48. Iyengar, S.S., LaFrancois, J.J., Friedman, D., Drew, L.J., Denny, C.A., Burghardt, N.S., Wu, M.V., Hsieh, J., Hen, R., and Scharfman, H.E. (2015). Suppression of adult neurogenesis increases the acute effects of kainic acid. Exp. Neurol. *264*, 135–149. https://doi.org/10.1016/j.expneurol.2014.11.009.

49. Lu, Y.M., Mansuy, I.M., Kandel, E.R., and Roder, J. (2000). Calcineurin-mediated LTD of GABAergic inhibition underlies the increased excitability of CA1 neurons associated with LTP. Neuron *26*, 197–205.

50. Wang, J., Liu, S., Haditsch, U., Tu, W., Cochrane, K., Ahmadian, G., Tran, L., Paw, J., Wang, Y., Mansuy, I., et al. (2003). Interaction of calcineurin and type-A GABA receptor gamma 2 subunits produces long-term depression at CA1 inhibitory synapses. J. Neurosci. *23*, 826–836.

51. Mehta, D., Ahmmed, G.U., Paria, B.C., Holinstat, M., Voyno-Yasenetskaya, T., Tiruppathi, C., Minshall, R.D., and Malik, A.B. (2003). RhoA interaction with inositol 1,4,5-trisphosphate receptor and transient receptor potential channel-1 regulates Ca2+ entry. Role in signaling increased endothelial permeability. J. Biol. Chem. *278*, 33492–33500. https://doi.org/10.1074/jbc.M302401200.

52. Kneussel, M., Brandstätter, J.H., Laube, B., Stahl, S., Müller, U., and Betz, H. (1999). Loss of postsynaptic GABA(A) receptor clustering in gephyrin-deficient mice. J. Neurosci. *19*, 9289–9297.

53. Essrich, C., Lorez, M., Benson, J.A., Fritschy, J.M., and Lüscher, B. (1998). Postsynaptic clustering of major GABAA receptor subtypes requires the gamma 2 subunit and gephyrin. Nat. Neurosci. *1*, 563–571.

54. Kreitzer, A.C., and Regehr, W.G. (2001). Cerebellar depolarization-induced suppression of inhibition is mediated by endogenous cannabinoids. J. Neurosci. *21*, RC174.

55. Llano, I., Marty, A., Armstrong, C.M., and Konnerth, A. (1991). Synaptic- and agonist-induced excitatory currents of Purkinje cells in rat cerebellar slices. J. Physiol. *434*, 183–213.

56. Burke, J.E., and Dennis, E.A. (2009). Phospholipase A2 structure/function, mechanism, and signaling. J. Lipid Res. *50*, S237–S242. https://doi.org/10.1194/jlr.R800033-JLR200.

57. Yegin, A., Akbas, S.H., Ozben, T., and Korgun, D.K. (2002). Secretory phospholipase A2 and phospholipids in neural membranes in an experimental epilepsy model. Acta Neurol. Scand. *106*, 258–262. https://doi.org/10.1034/j.1600-0404.2002.01238.x.

58. Johansen, A., Rosti, R.O., Musaev, D., Sticca, E., Harripaul, R., Zaki, M., Çağlayan, A.O., Azam, M., Sultan, T., Froukh, T., et al. (2016). Mutations in MBOAT7, encoding lysophosphatidylinositol acyltransferase I, lead to intellectual disability accompanied by epilepsy and autistic features. Am. J. Hum. Genet. *99*, 912–916. https://doi.org/10.1016/j.ajhg.2016.07.019.

59. Guy, A.T., Nagatsuka, Y., Ooashi, N., Inoue, M., Nakata, A., Greimel, P., Inoue, A., Nabetani, T., Murayama, A., Ohta, K., et al. (2015). Neuronal development. Glycerophospholipid regulation of modality-specific sensory axon guidance in the spinal cord. Science *349*, 974–977. https://doi.org/10.1126/science.aab3516.

60. Fletcher-Jones, A., Hildick, K.L., Evans, A.J., Nakamura, Y., Henley, J.M., and Wilkinson, K.A. (2020). Protein interactors and trafficking pathways that regulate the cannabinoid Type 1 receptor (CB1R). Front. Mol. Neurosci. *13*, 108. https://doi.org/10.3389/fnmol.2020.00108.

61. Devinsky, O., Patel, A.D., Thiele, E.A., Wong, M.H., Appleton, R., Harden, C.L., Greenwood, S., Morrison, G., and Sommerville, K.; GWPCARE1 Part A Study Group (2018). Randomized, dose-ranging safety trial of cannabidiol in Dravet syndrome. Neurology *90*, e1204–e1211. https://doi.org/10.1212/WNL.0000000000005254.

62. Marsicano, G., Goodenough, S., Monory, K., Hermann, H., Eder, M., Cannich, A., Azad, S.C., Cascio, M.G., Gutiérrez, S.O., van der Stelt, M.,

et al. (2003). CB1 cannabinoid receptors and on-demand defense against excitotoxicity. Science *302*, 84–88. https://doi.org/10.1126/science.1088208.

63. Sugaya, Y., and Kano, M. (2021). Endocannabinoid-mediated control of neural circuit excitability and epileptic seizures. Front. Neural Circuits *15*, 781113. https://doi.org/10.3389/fncir.2021.781113.
64. Farrell, J.S., Colangeli, R., Dong, A., George, A.G., Addo-Osafo, K., Kingsley, P.J., Morena, M., Wolff, M.D., Dudok, B., He, K., et al. (2021). In vivo endocannabinoid dynamics at the timescale of physiological and pathological neural activity. Neuron *109*, 2398–2403.e4. https://doi.org/10.1016/j.neuron.2021.05.026.
65. Evans, A.T., Formukong, E., and Evans, F.J. (1987). Activation of phospholipase A2 by cannabinoids. Lack of correlation with CNS effects. FEBS Lett. *211*, 119–122. https://doi.org/10.1016/0014-5793(87)81420-5.
66. White, H.L., and Tansik, R.L. (1980). Effects of delta 9-tetrahydrocannabinol and cannabidiol on phospholipase and other enzymes regulating arachidonate metabolism. Prostaglandins Med. *4*, 409–417. https://doi.org/10.1016/0161-4630(80)90049-x.
67. Bakas, T., van Nieuwenhuijzen, P.S., Devenish, S.O., McGregor, I.S., Arnold, J.C., and Chebib, M. (2017). The direct actions of cannabidiol and 2-arachidonoyl glycerol at GABAA receptors. Pharmacol. Res. *119*, 358–370. https://doi.org/10.1016/j.phrs.2017.02.022.
68. Bisogno, T., Hanus, L., De Petrocellis, L., Tchilibon, S., Ponde, D.E., Brandi, I., Moriello, A.S., Davis, J.B., Mechoulam, R., and Di Marzo, V. (2001). Molecular targets for cannabidiol and its synthetic analogues: effect on vanilloid VR1 receptors and on the cellular uptake and enzymatic hydrolysis of anandamide. Br. J. Pharmacol. *134*, 845–852. https://doi.org/10.1038/sj.bjp.0704327.
69. Qin, N., Neeper, M.P., Liu, Y., Hutchinson, T.L., Lubin, M.L., and Flores, C.M. (2008). TRPV2 is activated by cannabidiol and mediates CGRP release in cultured rat dorsal root ganglion neurons. J. Neurosci. *28*, 6231–6238. https://doi.org/10.1523/JNEUROSCI.0504-08.2008.
70. De Petrocellis, L., Ligresti, A., Moriello, A.S., Allarà, M., Bisogno, T., Petrosino, S., Stott, C.G., and Di Marzo, V. (2011). Effects of cannabinoids and cannabinoid-enriched cannabis extracts on TRP channels and endocannabinoid metabolic enzymes. Br. J. Pharmacol. *163*, 1479–1494. https://doi.org/10.1111/j.1476-5381.2010.01166.x.
71. Costa, B., Giagnoni, G., Franke, C., Trovato, A.E., and Colleoni, M. (2004). Vanilloid TRPV1 receptor mediates the antihyperalgesic effect of the nonpsychoactive cannabinoid, cannabidiol, in a rat model of acute inflammation. Br. J. Pharmacol. *143*, 247–250. https://doi.org/10.1038/sj.bjp.0705920.
72. Carrier, E.J., Auchampach, J.A., and Hillard, C.J. (2006). Inhibition of an equilibrative nucleoside transporter by cannabidiol: a mechanism of cannabinoid immunosuppression. Proc. Natl. Acad. Sci. USA *103*, 7895–7900. https://doi.org/10.1073/pnas.0511232103.
73. Ross, H.R., Napier, I., and Connor, M. (2008). Inhibition of recombinant human T-type calcium channels by Delta9-tetrahydrocannabinol and cannabidiol. J. Biol. Chem. *283*, 16124–16134. https://doi.org/10.1074/jbc.M707104200.
74. Rimmerman, N., Ben-Hail, D., Porat, Z., Juknat, A., Kozela, E., Daniels, M.P., Connelly, P.S., Leishman, E., Bradshaw, H.B., Shoshan-Barmatz, V., and Vogel, Z. (2013). Direct modulation of the outer mitochondrial membrane channel, voltage-dependent anion channel 1 (VDAC1) by cannabidiol: a novel mechanism for cannabinoid-induced cell death. Cell Death Dis. *4*, e949. https://doi.org/10.1038/cddis.2013.471.
75. Chamberland, S., Nebet, E., Rosenberg, E., Devinsky, O., and Tsien, R. (2019). Cannabidiol elevates the ratio of feedforward:feedback inhibition to dampen hippocampal activity propagation. Society for Neuroscience Annual Meeting, held in Chicago, United States.
76. Burman, R.J., Rosch, R.E., Wilmshurst, J.M., Sen, A., Ramantani, G., Akerman, C.J., and Raimondo, J.V. (2022). Why won't it stop? The dynamics of benzodiazepine resistance in status epilepticus. Nat. Rev. Neurol. *18*, 428–441. https://doi.org/10.1038/s41582-022-00664-3.
77. Goodkin, H.P., Joshi, S., Mtchedlishvili, Z., Brar, J., and Kapur, J. (2008). Subunit-specific trafficking of GABA(A) receptors during status epilepticus. J. Neurosci. *28*, 2527–2538. https://doi.org/10.1523/JNEUROSCI.3426-07.2008.
78. Loup, F., Wieser, H.G., Yonekawa, Y., Aguzzi, A., and Fritschy, J.M. (2000). Selective alterations in GABAA receptor subtypes in human temporal lobe epilepsy. J. Neurosci. *20*, 5401–5419.
79. Frugier, G., Coussen, F., Giraud, M.F., Odessa, M.F., Emerit, M.B., Boué-Grabot, E., and Garret, M. (2007). A gamma 2(R43Q) mutation, linked to epilepsy in humans, alters GABAA receptor assembly and modifies subunit composition on the cell surface. J. Biol. Chem. *282*, 3819–3828. https://doi.org/10.1074/jbc.M608910200.
80. Wallace, R.H., Marini, C., Petrou, S., Harkin, L.A., Bowser, D.N., Panchal, R.G., Williams, D.A., Sutherland, G.R., Mulley, J.C., Scheffer, I.E., and Berkovic, S.F. (2001). Mutant GABA(A) receptor gamma2-subunit in childhood absence epilepsy and febrile seizures. Nat. Genet. *28*, 49–52. https://doi.org/10.1038/ng0501-49.
81. Baulac, S., Huberfeld, G., Gourfinkel-An, I., Mitropoulou, G., Beranger, A., Prud'homme, J.F., Baulac, M., Brice, A., Bruzzone, R., and LeGuern, E. (2001). First genetic evidence of GABA(A) receptor dysfunction in epilepsy: a mutation in the gamma2-subunit gene. Nat. Genet. *28*, 46–48. https://doi.org/10.1038/88254.
82. Chuang, S.H., Westenbroek, R.E., Stella, N., and Catterall, W.A. (2021). Combined antiseizure efficacy of cannabidiol and clonazepam in a conditional mouse model of Dravet syndrome. J. J. Exp. Neurol. *2*, 81–85. https://doi.org/10.33696/neurol.2.040.
83. Anderson, L.L., Absalom, N.L., Abelev, S.V., Low, I.K., Doohan, P.T., Martin, L.J., Chebib, M., McGregor, I.S., and Arnold, J.C. (2019). Coadministered cannabidiol and clobazam: preclinical evidence for both pharmacodynamic and pharmacokinetic interactions. Epilepsia *60*, 2224–2234. https://doi.org/10.1111/epi.16355.
84. Gaston, T.E., Bebin, E.M., Cutter, G.R., Liu, Y., and Szaflarski, J.P.; Program, U.C. (2017). Interactions between cannabidiol and commonly used antiepileptic drugs. Epilepsia *58*, 1586–1592. https://doi.org/10.1111/epi.13852.
85. Geffrey, A.L., Pollack, S.F., Bruno, P.L., and Thiele, E.A. (2015). Drug-drug interaction between clobazam and cannabidiol in children with refractory epilepsy. Epilepsia *56*, 1246–1251. https://doi.org/10.1111/epi.13060.
86. Racine, R.J. (1972). Modification of seizure activity by electrical stimulation. I. After-discharge threshold. Electroencephalogr. Clin. Neurophysiol. *32*, 269–279. https://doi.org/10.1016/0013-4694(72)90176-9.
87. Gelinas, J.N., Khodagholy, D., Thesen, T., Devinsky, O., and Buzsáki, G. (2016). Interictal epileptiform discharges induce hippocampal-cortical coupling in temporal lobe epilepsy. Nat. Med. *22*, 641–648. https://doi.org/10.1038/nm.4084.
88. Van Erum, J., Van Dam, D., and De Deyn, P.P. (2019). PTZ-induced seizures in mice require a revised Racine scale. Epilepsy Behav. *95*, 51–55. https://doi.org/10.1016/j.yebeh.2019.02.029.
89. de Chaumont, F., Dallongeville, S., Chenouard, N., Hervé, N., Pop, S., Provoost, T., Meas-Yedid, V., Pankajakshan, P., Lecomte, T., Le Montagner, Y., et al. (2012). Icy: an open BioImage informatics platform for extended reproducible research. Nat. Methods *9*, 690–696. https://doi.org/10.1038/nmeth.2075.
90. Vandesompele, J., De Preter, K., Pattyn, F., Poppe, B., Van Roy, N., De Paepe, A., and Speleman, F. (2002). Accurate normalization of real-time quantitative RT-PCR data by geometric averaging of multiple internal control genes. Genome Biol. *3*. RESEARCH0034. https://doi.org/10.1186/gb-2002-3-7-research0034.

Please cite this article in press as: Rosenberg et al., Cannabidiol modulates excitatory-inhibitory ratio to counter hippocampal hyperactivity, Neuron (2023), https://doi.org/10.1016/j.neuron.2023.01.018

STAR★METHODS

KEY RESOURCES TABLE

REAGENT or RESOURCE	SOURCE	IDENTIFIER
Antibodies		
Rb α GPR55 1:500	Cayman Chemicals	Cat#10224; RRID:AB_10614518
MS α VGLUT1 1:100	Synaptic Systems	Cat#135 311; RRID:AB_887880
MS α VGAT 1:100	Synaptic Systems	Cat#131 011; RRID:AB_887872
GT α PSD-95 1:1000	Abcam	Cat#Ab12093; RRID:AB_298846
CK α Gephyrin 1:200	Abcam	Cat#Ab136343
MS α CB_1R 1:500	Synaptic Systems	Cat#258 011; RRID:AB_2619969
GP α Tau 1:1000	Synaptic Systems	Cat#314 004; RRID:AB_1547385
GP α MAP2 1:1000	Synaptic Systems	Cat#188 004; RRID:AB_2138181
RB α $GABA_AR$ $Gamma_2$ 1:500	Synaptic Systems	Cat#224 003; RRID:AB_2263066
RB α $GABA_AR$ $Gamma_2$ phospho-S327 1:500	Phospho-solutions	Cat#P1130-327; RRID:AB_2492116
RB α $GABA_AR$ $Beta_3$ 1:500	Synaptic Systems	Cat#224 404; RRID:AB_2619936
RB α $GABA_AR$ $Beta_3$ phospho-S408/409 1:500	Phospho-solutions	Cat#P1130-4089; RRID:AB_2492111
RB α Beta Actin 1:10,000	Cell Signaling	Cat#4970; RRID:AB_2223172
MS α GAPDH 1:10,000	GeneTex	Cat#GTX627408; RRID:AB_11174761
Chemicals, peptides, and recombinant proteins		
Y-27632	Cayman Chemicals	Cat#10005583
U 73122	Tocris	Cat#1268
Bisindolylmaleimide II	Tocris	Cat#4128
Thapsigargin	Tocris	Cat#1138
(-)-Xestospongin C	Cayman Chemicals	Cat#64950
Cyclosporin A (CsA)	Tocris	Cat#1101
Tautomyectin	Tocris	Cat#2305
CID16020046	Cayman Chemical	Cat#15247
AACOCF3	Cayman Chemical	Cat#62120
YM 26734	Cayman Chemical	Cat#17631
Highly purified cannabidol (CBD)	GW Research Ltd, Cambridge, UK	Materials Agreement
L- α lysophosphatidylinositol sodium salt from soybean	Sigma	Cat#62966
Tetrodotoxin	Tocris	Cat#1078
NBQX	Tocris	Cat#1044
D-APV	Tocris	Cat#0106
AM281	Sigma	Cat#A0980
Pentylenetetrazole	Sigma	Cat#P6500
Kainic acid	Sigma	Cat#K0250
Experimental models: Organisms/strains		
GPR55 KO Mouse (*B6;129S-Gpr55^{tm1Lex}/Mmnc*)	Professor Ken Mackie, Indiana University	Gift; RRID:MMRRC_030008-UNC
C57Bl/6J Mouse	Jackson Laboratory	Strain#000664; RRID:IMSR_JAX:000664
Sprague-Dawley Rat	Charles River	Strain#400
(PV)-Cre Mouse (*B6;129P2-Pvalb$^{tm1(cre)Arbr}$/J*)	Jackson Laboratory	Strain#017320; RRID:IMSR_JAX:017320
Ai9/TdTomato Mouse (*B6.Cg-Gt(ROSA) 26Sor$^{tm9(CAG-tdTomato)Hze}$/J*)	Jackson Laboratory	Strain#007909; RRID:IMSR_JAX:007909
Ai32-channelrhodopsin 2 EYFP Mouse (*B6;Cg-Gt(ROSA)26Sor$^{tm32(CAG-COP4*H134R/EYFP)Hze}$/J*)	Jackson Laboratory	Strain#024109; RRID:IMSR_JAX:024109

(*Continued on next page*)

Please cite this article in press as: Rosenberg et al., Cannabidiol modulates excitatory-inhibitory ratio to counter hippocampal hyperactivity, Neuron (2023), https://doi.org/10.1016/j.neuron.2023.01.018

Continued

REAGENT or RESOURCE	SOURCE	IDENTIFIER
Wistar-Kyoto Rats	Charles River	Strain#008
Swiss Mice	Taconic	Strain#SW-M
Oligonucleotides		
5'-TGAGTCAGCTAGA	Origene	Custom Designed
CAGTAACAACTGCTCG-3'	Origene	Custom Designed
5'-CAACCTGGCTGTCTT	Origene	Custom Designed
CGACTTACTGCTTG-3'	Origene	Custom Designed
5'-CTGGACCATTGCTAC	Origene	Custom Designed
CAATCTTGTCGTCT-3'	Origene	Custom Designed
5'-CTCAATGTAGTTCAG	Origene	Custom Designed
CCATAGCAGAATGA-3'	Origene	Custom Designed
Recombinant DNA		
mHmbs-qPCRF (mouse) GAGAAAGTTCCCCCACCTGG	Genewiz	Custom Designed
mHmbs-qPCRR (mouse) CCAGGACGATGGCACTGAAT	Genewiz	Custom Designed
mSdha-qPCRF (mouse) TGCGGCTTTCACTTCTCTGT	Genewiz	Custom Designed
mSdha-qPCRR (mouse) CGCCTACAACCACAGCATCA	Genewiz	Custom Designed
mGpr55-qPCRF (mouse) GCTTGGGGACAGAAGTGTGA	Genewiz	Custom Designed
mGpr55-qPCRR (mouse)gctgcaaggttc tggtaagc	Genewiz	Custom Designed
rHmbs-qPCRF (rat) GGACCTGGTTGTTCACTCCC	Genewiz	Custom Designed
rHmbs-qPCRR (rat) GGCAAGGTTTCCAGGGTCTT	Genewiz	Custom Designed
rSdha-qPCRF (rat) CGCTCACATACTGTTGCAGC	Genewiz	Custom Designed
rSdha-qPCRR (rat) TCAGAGCCTTTCACGGTGTC	Genewiz	Custom Designed
rGpr55-qPCRF2 (rat) TCAGCCCGAGAAGGAACTGCTTC	Genewiz	Custom Designed
rGpr55-qPCRR2 (rat) TGGTCAGGTTGTCCACGAAAACGAA	Genewiz	Custom Designed
Software and algorithms		
pClamp 9	Molecular Devices	https://www.moleculardevices.com//
Prism	GraphPad	https://www.graphpad.com/
MATLAB	Mathworks	https://www.mathworks.com/
Icy	Institut Pasteur/ France Bioimaing	https://icy.bioimageanalysis.org
Colocalization Analysis	This paper	Github: https://github.com/ecr305/punctacolocalization
Electrophysiology Analysis	This paper	Github: https://github.com/ecr305/ephysanalysis

RESOURCE AVAILABILITY

Lead contact

Further information and requests for resources and reagents should be directed to and will be fulfilled by the lead contact, Richard Tsien (Richard.tsien@nyulangone.edu).

Please cite this article in press as: Rosenberg et al., Cannabidiol modulates excitatory-inhibitory ratio to counter hippocampal hyperactivity, Neuron (2023), https://doi.org/10.1016/j.neuron.2023.01.018

Materials availability

- No unique plasmids suitable for deposition have been generated in this study. shRNA targeting *Gpr55* was generated through Origene, using sequences as listed in methods below. Primers for *Gpr55* qPCR were generated through Genewiz, using sequences as listed in methods below.
- No unique mouse lines have been generated in this study. GPR55 KO (*B6;129S-Gpr55*^{tm1Lex}*/Mmnc*) mice were generously provided by Prof. Ken Mackie, Indiana University (kmackie@indiana.edu).
- This study did not generate any new unique agents.

Data and code availability

- All primary data reported in this study will be shared by the lead contact upon request.
- All original code used for data analysis has been deposited at Github and is publicly available as of the date of publication. DOIs are listed in the key resources table.
- Any additional information required to reanalyze the data reported in this work paper is available from the lead contact upon request.

EXPERIMENTAL MODEL AND SUBJECT DETAILS

Animals

All procedures involving animals were approved by the Institutional Animal Care and Use Committee at the New York University Langone Medical Center, and in accordance with guidelines from the US National Institutes of Health. GPR55 KO (*B6;129S-Gpr55*^{tm1Lex}*/Mmnc*) mice were generously provided by Prof. Ken Mackie, Indiana University, and backcrossed to a C57Bl/6JC57BL/6J (WT, +/+, Jax Strain #000664) background at NYU to expand the colony. Both male and female GPR55 KO and WT mice age P24-P90 were used for experiments as further described in the methods below. For cell culture experiments, male and female SAS Sprague-Dawley rat (Charles River #400) P0 pups were utilized. PV interneurons were identified with parvalbumin (PV)-Cre (*B6;129P2-Pvalb*$^{tm1(cre)Arbr}$*/J,* Jax Strain #017320) line crossed with a Ai9/TdTomato expressing lines (*B6.Cg-Gt(ROSA)26Sor*$^{tm9(CAG-tdTomato)Hze}$*/J,* Jax Strain #007909). For optogenetic experiments involving PV+-mediated inhibition, PV-Cre mice were crossed with an Ai32 line expression channelrhodopsin 2 EYFP fusion protein (*B6;Cg-Gt(ROSA)26Sor*$^{tm32(CAG-COP4*H134R/EYFP)Hze}$*/J*, Jax Strain #024109). For transgenic mice experiments in PV-Ai9 and PV-Cre/Ai32/ChR2 mice, both male and female mice age P60-90 were used for electrophysiological experiments.

Male Wistar-Kyoto rats (>P21, Charles River #008) were used for studies involving lithium pilocarpine-induced status epilepticus at the University of Aston (UK). All rats were maintained in 12h:12h dark:light cycle, a room temperature of 21°C and humidity of 50±10 %, with *ad libitum* access to food and water. The experiments were performed in accordance with UK Home Office regulations (Animals Scientific Procedures Act, 1986). Male Swiss mice weighing 18–25g (Taconic, Germantown, NY, Model SW-M) were used for electrographic pentylenetetrazole (PTZ)-induced seizures (Figure 7) as previously described.[44]

Primary Cell Cultures

Hippocampal neurons were cultured from postnatal day 0 male and female Sprague-Dawley rat pups. The hippocampus was isolated in ice-cold HBSS (Corning) containing 20% fetal bovine serum (FBS), and washed in HANKS without serum. Following washing, hippocampi were digested for 8 min. in a 1 ml papain solution (Papain dissociation System, Worthington). 50 units of DNase I (Millipore Sigma) and 0.5 μM $MgCl_2$ was added at the end of Papain digestion. Digestion was stopped by adding 5 ml of modified HBSS containing 20% fetal bovine serum. After additional washing, the tissue was dissociated using Pasteur pipettes of decreasing diameter. The cell suspension was pelleted and plated on 10 mm coverslips coated with poly-D-lysine in 24-well plates for ICC, or directly onto PDL-coated 12 well plates for western blot studies. The cultures were maintained in NbActiv4 (BrainBits, Springfield, IL). A 50% medium change was performed at 7 days, and once per week thereafter. Neurons were used for experiments 12-14 days in vitro (DIV) after plating.

METHOD DETAILS

Induction of pentylenetetrazole (PTZ)-induced seizures in mice (Figure 1)

During a pre-experimental baselining period, animals were randomized for treatment, and treatment groups were balanced within litters to the extent permitted by individual litter size, sex, and genotype distribution. Male GPR55$^{+/+}$ (n=40) and GPR55$^{-/-}$ (n=40) mice, aged P24-28 and weighting 25–40g, were injected intraperitoneally (i.p.) with vehicle (ethanol: kolliphor®: 0.9% saline=1:1:18; Sigma-Aldrich, UK) 1h before receiving i.p. administration of PTZ (Sigma-Aldrich, UK) at 85, 95, 105 or 115 mg/kg (n=10 per group) dissolved in saline (0.9% (w/v) NaCl). During the 30 min following PTZ injection, the number of animals exhibiting fully developed tonic-clonic seizures with loss of righting reflex and/or death was calculated.

The acute experimental phase of the study utilized a similar design, but included administration of plant-derived, highly purified cannabidiol (CBD, generously provided by GW Research Ltd, Cambridge, UK) at doses of 50, 100, or 200 mg/kg, or vehicle, given 30 min before injection of PTZ (105 mg/kg i.p.) or vehicle. Animals were sacrificed within 30 min of PTZ injection or if premature death occurred following status epilepticus.

EEG recordings and analysis for high dose PTZ Seizures (Figure 1; Figure S1)

Implants

Mice (n=3 WT, n=3 GPR55 KO, 3–4 months old, male) were anesthetized with 1.5-2% isoflurane (2 L/min) and provided with a local anesthetic to the incision site (bupivicaine at 0.5 mg/kg, 2.5 mg/ml, s.c.). The skull was cleaned with saline and hydrogen peroxide, and ground wires (bare stainless steel) were positioned intracranially over the cerebellum. The skull was then coated with Optibond (Kerr Dental, Brea, CA) and a craniotomy (~0.25 x 0.25 mm) was performed at AP -2.2, ML -2.0 (left hemisphere). The dura was pierced, and the tungsten wires were implanted ~0.9mm into the brain. The wires with custom driver were cemented to the skull with C & B Metabond Quick Adhesive Cement (Parkell) and Unifast Trad acrylic (GC America). The craniotomy was capped with a mixture of mineral oil (one part) and dental wax (three parts), and a Faraday cage was constructed using copper mesh and connected to the cerebellar ground wire. Following surgery, an opioid analgesic was injected (Buprenex at 0.06 mg/kg, 0.015 mg/ml, i.m.) and given as needed for the next 1-3 days.

Recording

Three insulated tungsten wires (0.002'' California Fine Wire, CA) were glued together and cut at a 45º angle. These were then mounted to a screw and soldered to a header pin (Mill-Max, NY). Signals were digitized at 30 KHz with the Intan amplifier board (RHD2132/RHD2000 Evaluation System, Intan). Mice were allowed at least a one week post-implantation recovery before electrodes were lowered into place. CA1 ripples (150 – 200Hz oscillation) were used to identify correct placement prior to experimentation. At least one day was allowed between electrode placements and seizure induction. On the day of seizure induction, mice were placed in their home cage, and the position was monitored by a USB webcam synchronized with the neural recordings through a blinking LED. First, CBD (200 mg/kg i.p.) was injected, followed 1 h later by injection of PTZ (105 mg/kg i.p.). Recordings were made for at least 30 minutes or until death.

Analysis

Behaviorally observed seizure state was classified independently based on neural activity and on behavior using the Racine scale.[86] Electrographic events were characterized in 30 second time blocks as one of four classifications: **(***1) Normal*: normal EEG background without epileptiform discharges, seizures, or slowing; *(2) Epileptiform discharges*[87] clusters of >2 spikes, with absolute value of LFP amplitude larger than 4 standard deviations of the LFP recorded throughout, spike duration less than 75 ms in duration as measured by the width at half max, and no evolution over the duration of 30 s time window; **(***3) Seizures*[88] high amplitude, rhythmic trains of high frequency complex discharges lasting for a minimum of 5 s; (4) *Post-ictal suppression*: LFP values in the bottom decile of LFP values recorded throughout the experiment. Spectrograms were made in MATLAB v2018b (Mathworks, MA) using Morlet wavelets on the down-sampled (1250 Hz) local field potential from the recording site with the largest amplitude ripples.

Induction of lower dose pentylenetetrazole (PTZ)-induced seizures in mice (Figure 6)

Methods were performed as previously described.[44] In brief, male Swiss Mice weighing 18-25 g (Taconic, Germantown, NY) were used. Four total electrodes were placed over left frontal, right occipital and bilateral hippocampi. Animals were treated subcutaneously (s.c.) with either vehicle (ethanol: kolliphor®: 0.9% saline=1:1:18; Sigma-Aldrich, UK) or 200 mg/kg CBD (plant-derived highly purified, generously provided by GW Research Ltd, Cambridge, UK). One hour later, animals were injected with pentylenetetrazol (60 mg/kg s.c.; Sigma-Aldrich, UK). During seizure induction, mice were monitored using a webcam synchronized with the EEG recordings. Seizure behavior was analyzed by a blinded observer using Racine scale as described.[86] Electrographic activity was analyzed with Sirenia (v2.2.1; Pinnacle) or Spike 2 (v7.12; Cambridge Electronics). Recordings were analyzed for latency to the first abnormal event (epileptiform activity or seizure), seizure duration, and power. Power Spectrograms were made in MATLAB (v2018b; Mathworks, MA) using Morlet wavelets of the down-sampled (1250 Hz) EEG from the recording site.

Induction of chronic epilepsy in Wistar-Kyoto rats

Using a recently described model of low-mortality, high-morbidity status epilepticus,[46] male (P>21) Wistar-Kyoto rats (Charles River) were injected subcutaneously (s.c.) with lithium-chloride (127 mg/kg) 24 hours before pilocarpine treatment, to sensitize them to the seizurogenic effects of pilocarpine. 30 minutes prior to pilocarpine treatment, animals were injected with methylscopolamine (Sigma-Aldrich, UK; 1 mg/kg; s.c.), a peripherally restricted muscarinic receptor antagonist that minimizes the peripheral effects of pilocarpine (salivation etc.). Pilocarpine (Sigma-Aldrich, UK; 25 mg/kg; s.c.) was administered at 30-min intervals until bilateral rearing and falling (Racine stage 3.5) was observed. Xylazine (Sigma-Aldrich, UK; 2.5 mg/kg; s.c.) was then injected to inhibit motor movement during seizures. Following 60 minutes of sustained seizure activity, animals were injected with ''STOP'' solution (1 ml/kg; s.c.), consisting of diazepam (Sigma-Aldrich, UK; 2.5 mg/kg), 2-methyl-6-(phenylethynyl) pyridine (Sigma-Aldrich, UK; 20 mg/kg), and dizoclipine (MK-801; Sigma-Aldrich, UK; 0.1 mg/kg) to prevent further seizures. During the 2 weeks after induction, regular animal welfare checks were performed. Epileptogenesis was determined using a previously validated post-seizure behavioral battery

Please cite this article in press as: Rosenberg et al., Cannabidiol modulates excitatory-inhibitory ratio to counter hippocampal hyperactivity, Neuron (2023), https://doi.org/10.1016/j.neuron.2023.01.018

(PSBB) test, and only animals with PSBB scores >10 following a 10 week period were used for electrophysiology and IHC.[46] In the weeks following the establishment of epileptogenesis, rats were randomly divided into two groups to receive either 200 mg/kg CBD or vehicle (3.5% kolliphor ® HS, Sigma) as per.[14] All drugs were administered in drinking water to reduce the incidence of spontaneous seizures with epileptic animals during frequent handling.

Two-Pulse Kainic Acid (KA) Seizure Induction

For the "KA1" pulse, WT C57Bl6 mice (2–3 months, male and female) received either CBD (200 mg/kg) or CBD vehicle (ethanol: kolliphor®: 0.9% saline=1:1:18; Sigma-Aldrich), followed by kainic acid (KA, Sigma, 24 mg/kg in normal saline, s.c.) 1 h later. Behavioral seizures were then scored based on a modified Racine scale[86]: 0 – Grooming, moving, normal; 1 – Freezing, splayed limbs, sloppy movements; 2 – Ear twitching, head nodding; 3 - Unilateral arm jerks; 4 - Bilateral arm jerks, with stages 3-4 identifying convulsive seizures. Animals were then given diazepam (Hospira, Inc, 10 mg/kg, s.c.) 2 hours later to prevent status epilepticus. For qPCR experiments, 48 h following KA1 injection, animals were sacrificed and brains were rapidly frozen for mRNA extraction. For those receiving the "KA2" pulse, 48 h following KA1, a second dose of CBD or vehicle (concentrations as above), followed by KA (as above) was given. Behavioral seizures were again assayed as per the modified Racine Scale.

Electrophysiology slice preparation (for mice, all except Figure 7)

GPR55 KO or littermate control mice 2-3 months old, male and female, were anesthetized with a mixture of ketamine/xylazine (150 mg/kg and 10 mg/kg, respectively) and perfused transcardially with an ice-cold sucrose solution containing (in mM): 206 Sucrose, 11 D-Glucose, 2.5 KCl, 1 NaH_2PO_4, 10 $MgCl_2$, 2 $CaCl_2$ and 26 $NaHCO_3$. Following perfusion and decapitation, brains were removed and placed in the cold sucrose for sectioning before gluing to the stage of a Leica VT 1000S Vibratome. Transverse, 350 μm sections of left and right hippocampi were cut and transferred to an oxygenated, 34°C recovery chamber filled with artificial cerebrospinal fluid (ACSF) containing (in mM): 122 NaCl, 3 KCl, 10 D-Glucose, 1.25 NaH_2PO_4, 2 $CaCl_2$, 1.3 $MgCl_2$, and 26 $NaHCO_3$. Slices were allowed to recover for 1 h at 34°C and were then maintained at room temperature in oxygenated ACSF for 1-6 h before recording.

Electrophysiological recordings (for mice, all except Figure 7)

Hippocampal slice recordings were performed in a submerged chamber maintained at 32-34°C with a constant bath perfusion of ACSF (with or without pharmacological agents) at ~4 mL/min. Slices equilibrated in the chamber for >10 minutes before recording. Whole cell and cell-attached recordings were made with borosilicate glass pipettes pulled on a Sutter Instrument P-97 micropipette puller. Tip resistance ranged between 2-5 MΩ following fire polishing to enhance seal quality.

For voltage clamp recordings of spontaneous and evoked EPSCs, the intracellular solution contained (in mM): 130 CsMeSO3, 6 CsCl, 1 MgCl2, 10 HEPES, 0.3 EGTA, 10 Tris-Phosphocreatine, 4 Mg-ATP and 0.3 Na-GTP. Spontaneous IPSCs onto pyramidal cells were recorded in voltage clamp using a high Cl- internal solution containing (in mM): 70 $CsMeSO_3$, 35 CsCl, 15 TEA-Cl, 1 $MgCl_2$, 0.2 $CaCl_2$, 10 HEPES, 0.3 EGTA, 10 Tris-Phosphocreatine, 4 Mg-ATP and 0.3 Na-GTP, with ACSF glutamatergic blockers 10μM NBQX and 50 μM APV. For mEPSC and mIPSC recordings, 1μM TTX was added to ACSF. For disynaptic IPSC experiments, cells were held at 0mV and stabilized for at least 10-15 minutes prior to recording. For synaptic stimulation recordings, stimulating electrodes were placed in the *stratum radiatum*, and a 10x 10Hz frequency train was delivered, with either 15s (eEPSCs) or 30s (eIPSCs) between trains.

Whole-cell patch clamp recordings were performed on neurons in the CA1 region of the hippocampus, identified visually with an upright microscope (Zeiss Axioskop 2 FS Plus) using infrared differential interference contrast (IR-DIC) optics. For all experiments involving lysophosphatidylinositol (LPI) application, cells were recorded in regular ACSF for 10-15 minutes, followed by LPI (4 μM, Sigma in DMSO vehicle) for 30 minutes, and a subsequent 10-15 minute washout period. In a subset of experiments, plant-derived highly purified CBD (GW Research Ltd, Cambridge, UK, 1μM in DMSO vehicle) was added for 20 minutes prior to concomitant LPI treatment (CBD+LPI).

Data were recorded with a MultiClamp 700B amplifier (Axon Instruments), filtered at 10 kHz using a Bessel filter and digitized at 20 kHz with a Digidata 1322A analogue-digital interface (Axon Instruments). mEPSCs and mIPSCs were analyzed using Clampfit software, and evoked EPSCs/IPSCs were identified offline using a custom analysis script developed in MATLAB (Mathworks). Passive properties were continuously monitored during recordings, and all cells with V_m <-55 mV, Series Resistance (R_s) > 25MΩ, or significant changes in R_s during the course of the recording, were excluded from analysis.

Electrophysiology slice preparation (for rats, Figure 7 only)

Healthy and epileptic male rats (p>66) were decapitated under deep isoflurane anaesthesia (4%$^{w}/_{v}$ in O_2), and their brains were rapidly removed and placed in ice-cold artificial cerebrospinal fluid (ACSF) solution containing (in mM): 130 NaCl, 24 $NaHCO_3$, 3.5 KCl, 1.25 NaH_2PO_4, 2.5 $CaCl_2$, 1.5 $MgSO_4$, 10 glucose saturated with 95% O_2, 5% CO_2, at pH 7.3. Transverse slices (350 μm thickness) including hippocampus were cut using a Vibroslice (Campden instruments Ltd., Loughborough, Leicestershire, UK) and transferred to a nylon mesh where they were maintained submerged in a chamber containing ACSF at 33°C for 30 min. Slices were then maintained at room temperature (18-22°C) in ACSF (95% O_2 / 5% CO_2).

Please cite this article in press as: Rosenberg et al., Cannabidiol modulates excitatory-inhibitory ratio to counter hippocampal hyperactivity, Neuron (2023), https://doi.org/10.1016/j.neuron.2023.01.018

Acute slices were secured under a nylon mesh, submerged, and superfused with ACSF in a chamber mounted on the stage of an upright microscope (Scientifica, UK). Slices were visualized with a 40×/0.1 NA water-immersion objective coupled with infrared and differential interference contrast (DIC) optics linked to a video camera (digital camera Orca 03G, Hamamatsu, Hamamatsu City, Japan).

Electrophysiological recordings (for rats, Figure 7 only)

Somatic whole-cell patch-clamp recordings (at ~33°C) were made from visually identified cells using borosilicate glass capillaries (GC150F-10; Harvard Apparatus Ltd., Kent, UK) using a P1000 Flaming Brown Micropipette puller (Sutter Instruments Co., California, USA) and filled with a filtered intracellular solution consisting of (in mM): 120 K-gluconate, 4 KCl, 4 Mg-ATP, 10 HEPES, 0.3 Na_2-GTP, 10 Na_2-phosphocreatine, pH adjusted to 7.2 with KOH. Resistance of the patch pipettes was 5-6 MΩ. Recordings were accepted only if the initial seal resistance was >1 GΩ and series resistance did not change by more than 20% throughout the recording period. No correction was made for the junction potential between the pipette and the ACSF. Pyramidal neurons were distinguished from interneurons by the localization of their somata in CA1 *stratum pyramidale*, a lower input resistance, a higher membrane constant, a smaller fast after-hyperpolarization and adapting, <20 Hz maximum firing rates. Intracellular signals were digitised to a computer with an A–D converter (Digidata 1500, Molecular Devices) and monitored during experiments with Clampex software (Molecular Devices). All electrophysiological signals were amplified (Multiclamp 700B, Molecular devices), low pass filtered at 10 kHz, digitized at 20 kHz.

In recordings of miniature excitatory postsynaptic currents (mEPSCs; voltage-clamp), the AMPA receptor component was isolated by adding 0.1 μM CGP 55845 (Abcam, UK), 100 μM D-APV (Abcam, UK), 500 μM MCPG (Abcam, UK), 1 μM strychnine (Sigma Aldrich, UK), 20 μM Bicuculline (Abcam, UK), 500 nM AM281 (Sigma Aldrich, UK) and 1 μM TTX (Tocris, UK) in the ACSF. GPR55 receptors were activated by applying 4 μM LPI (Sigma Aldrich, UK). In some experiments plant-derived highly purified CBD (GW Research Ltd, Cambridge, UK) was added to the ACSF at a final concentration of 1 μM. The DMSO concentration never exceeded 0.01%$^{w}/_{v}$.

Two-Photon Calcium Imaging

To image GCaMP6f confined to PV+ interneuron terminals (Figure S2E) we used acute hippocampal slices derived from male PV-Cre x Ai148 mice. Images were focused at the *stratum pyramidale* and *stratum radiatum* in the CA1 hippocampus. The field of view was imaged at 30 Hz by using a resonant scanner-based two-photon microscope (Sutter), and individual frames were subsequently averaged before analysis. 4 μM LPI was washed onto slices for ~3 min, followed by 25 mM KCl for ~1 min as a positive control to ensure the integrity of axon terminals to flux Ca^{2+}. Calcium responses were measured as a ratio of $\Delta F/F_0$, with F_0 representing basal fluorescence measured before LPI application.

Cell Culturing

A subset of cultures were transfected at 3DIV (MOI=5) with 4 custom designed lentiviral, GFP+ shRNA constructs (Origene) targeting GPR55 with the following sequences, along with scrambled controls:

5'-TGAGTCAGCTAGACAGTAACAACTGCTCG-3'
5'-CAACCTGGCTGTCTTCGACTTACTGCTTG-3'
5'-CTGGACCATTGCTACCAATCTTGTCGTCT-3'
5'-CTCAATGTAGTTCAGCCATAGCAGAATGA-3'

Immunostaining

For all cell culture experiments involving LPI treatment, cells were treated for 1 hour with pre-warmed 4mM K Tyrode's solution consisting of (in mM): 150 NaCl, 4 KCl, 2 $MgCl_2$, 2 $CaCl_2$, 10 HEPES, 10 glucose, pH 7.4, and synaptic blockers 1μM TTX, 10μM NBQX, and 50 μM APV. 4μM LPI, or DMSO vehicle, was then applied in Tyrode's solution with synaptic blockers. Cultured cells were then fixed at 30 or 60 minutes post drug application in ice-cold 4% paraformaldehyde in PBS supplemented with 20 mM EGTA and 4% (w/v) sucrose. Fixed cells were then permeabilized with 0.1% Triton X-100, blocked with 5% normal donkey serum, and incubated overnight with primary antibodies (see table below). The next day, cells were washed with PBS, incubated at room temperature for 50 min with Alexa secondary antibodies (1:1000, Molecular Probes), washed with PBS (3x5 min) and mounted using with ProLong Gold Antifade Mountant with or without DAPI (ThermoFisher Scientific).

For all experiments involving *ex vivo* hippocampal brain slices, animals were perfused with PBS followed by 4% paraformaldehyde in PBS. Whole brains were dissected and fixed overnight in 4% PFA, and then sucrose-protected overnight in 30% sucrose in PBS before embedding and freezing in optimal cutting temperature compound (Tissue-Tek O.C.T.) for sectioning. Frozen sections were cut on a cryostat at 16 μm and collected on HistoBond coated slides (VWR) for staining. Sections were blocked for 2-3 hours at room temperature in 0.2% Triton X-100 and 5% normal serum, then incubated at 4°C in primary antibodies (see chart below).

Please cite this article in press as: Rosenberg et al., Cannabidiol modulates excitatory-inhibitory ratio to counter hippocampal hyperactivity, Neuron (2023), https://doi.org/10.1016/j.neuron.2023.01.018

Sections were rinsed and then incubated in species-appropriate Alexa Fluor conjugated secondary antibodies (Molecular Probes, 1:500) for 2-3 hours, and finally mounted with ProLong Gold Antifade Mountant with or without DAPI (ThermoFisher Scientific). Fluorescent images were acquired on a Zeiss LSM 510 meta Imager.M1 confocal microscope at 10x, 20x, or 63x magnification.

Images were analyzed for both average puncta intensity and colocalization using custom analysis scripts in Icy (http://icy.bioimageanalysis.org) software.[89] Regions of interest (ROI) were traced around apical dendrites labeled by MAP2 or axons labeled by tau. For puncta colocalization analyses, immunoreactive puncta for GPR55 and synaptic markers (e.g. VGLUT1, VGAT) were separately detected with sub-pixel accuracy, in 3D, and in an automated manner using the 'Spot Detector' plugin of ICY (scale 2, threshold = 100). Puncta were determined to be "colocalized" with a threshold of 250 nm in the horizontal (XY) plane and 500 um in the depth (Z) plane, based on average pixel sizes of 120 nm XY and 370 nm Z, respectively. The 3D colocalization ratio was then computed as: (#colocalized GPR55 puncta + #colocalized marker puncta)/(total # GPR55 puncta + total #marker puncta). In order to gain a statistical insight on the estimated correspondence between puncta, we adopted a Monte Carlo simulation approach in which we aimed at building the probabilistic distribution of the colocalization ratio under the null hypothesis that the protein GPR55 is uniformly distributed along the axon and that colocalization with synaptic markers occurs only by chance. We randomly redistributed the location of GPR55 immunoreactive puncta along the axon in 2D after detection, while keeping their number fixed. Briefly, using the tau (axonal) or MAP2 (dendritic) fluorescence ROIs in 2D, we traced a series of linked 2D segments and orthogonally projected the detections for the two proteins along them so that a detection with 3D coordinates (x, y, z) is then represented by a single value (t) corresponding to the 1D distance to the tip of the traced axon/dendrite. We then computed the colocalization ratio as before in this coordinate system (colocalization threshold = 250 nm). For simulated data, we performed 10^4 trials in which the location of synaptic marker puncta remained fixed to preserve the spatial distribution of the protein, while GPR55 detections were randomly uniformly redistributed along the axonal segment. For each axonal segment, we compared the averaged simulated colocalization ratio with the measured one and we statistically pooled data from multiple coverslips using a paired t-test.

Immunoblotting

Cells were harvested and lysed (Lysis Buffer A, Thermo) with EDTA-free protease and phosphatase inhibitors (Thermo) following treatment with 4μM LPI (see immunostaining above for description). In a subset of studies, samples were treated with pharmacological blockers (see table below), and lysed at various times post LPI application. Sample proteins were equalized using the BCA Protein Assay Kit (Pierce) and loaded into 10-20% SDS-PAGE gel with 5% beta-mercaptoethanol following heating at 95°C for 5 min. Cellular protein was transferred to Immobilon transfer membrane (Millipore). The membrane was then blocked at room temperature for 2 hrs in Odyssey blocking buffer (Li-Cor Biosciences, Lincoln, NE), and incubated with primary antibodies (see table below). The following day, the membrane was washed with 0.1% Tween 20 in PBS and incubated with an IRDye-labeled secondary antibody (Li-Cor) for 1 hr. After incubation, the membrane was washed with PBS and imaged with Odyssey imaging systems. All the bands were analyzed with Image Studio software.

Total RNA extraction and qPCR

For the PTZ (105mg/kg, i.p.)-induced seizure model, one hippocampus was dissected out on ice and used for total RNA extraction at the time point either immediately after seizure-induced death, or 30 minutes after PTZ/vehicle treatment, whichever came first. For KA-induced seizure model, one hippocampus was dissected out on ice 48 hours following either KA (24 mg/kg, i.p., "KA1") or vehicle. For both PTZ and KA experiments, CBD (200 mg/kg) was administered 1 h prior to chemoconvulsant induction in a subset of animals. RNeasy Mini Kit (Qiagen, Cat#74104) was used to extract total RNA as per manufacturer instructions. Total RNA was eluted in 30 μl of RNase-free water and concentration was measured using nanodrop. SuperScript III Reverse Transcriptase (ThermoFisher Scientific #18080044) was used for reverse transcription of 1 μg (for the PTZ experiments) or 500 ng (for the KA experiments) total RNA from each sample following the user manual. qPCR was performed with SsoAdvanced Universal SYBR Green Supermix (Bio-Rad# 1725272) using 1 μl cDNA as template. Mouse *Gpr55* qPCR primers were designed to span an intron and were confirmed with non-RT control to make sure there is no genomic DNA interference (Figures S7A and S7B), and all PCR products were confirmed by Sanger sequencing. Two internal control genes (*Hmbs* and *Sdha*) were used with geometric averaging to ensure accurate normalization.[90]

For the qPCR assay of Li-PLC-induced seizure model in rats, hippocampi were dissected 3-6 months following establishment of epileptogenesis with age-matched non-epileptic controls, and flash frozen in liquid nitrogen. One half of a hippocampus (~30 mg) from each rat was used to extract total RNA using the RNeasy Mini Kit. To eliminate genomic DNA contamination, column-purified RNA were treated with RNase-free DNase I (Ambion, AM2224) at 37 °C for 30 minutes followed by 75°C inactivation for 10 minutes and column cleaning. Non-RT controls, in which no reverse transcriptase was added in the reverse transcription reaction, were run for all samples to monitor the level of genomic DNA contamination in the case of all-isoform *Gpr55* qPCR. We tested different promoter usages of rat *Gpr55* and used primer 10&11 (below) in Figure 7B.

Primers used for qPCR:

Please cite this article in press as: Rosenberg et al., Cannabidiol modulates excitatory-inhibitory ratio to counter hippocampal hyperactivity, Neuron (2023), https://doi.org/10.1016/j.neuron.2023.01.018

ID	Primer	Sequence	Notes
1	mHmbs-qPCRF	GAGAAAGTTCCCCCACCTGG	1&2: mouse internal control 1
2	mHmbs-qPCRR	CCAGGACGATGGCACTGAAT	
3	mSdha-qPCRF	TGCGGCTTTCACTTCTCTGT	3&4: mouse internal control 2
4	mSdha-qPCRR	CGCCTACAACCACAGCATCA	
5	mGpr55-qPCRF	GCTTGGGGACAGAAGTGTGA	5&6: mouse *Gpr55*, flanking intron; isoform-specific; (Figure 6C; Figures S7A and S7B)
6	mGpr55-qPCRR	GCTGCAAGGTTCTGGTAAGC	
7	ratHmbs-qPCRF	GGACCTGGTTGTTCACTCCC	7&8: rat internal control 1
8	ratHmbs-qPCRR	GGCAAGGTTTCCAGGGTCTT	
9	ratSdha-qPCRF	CGCTCACATACTGTTGCAGC	9&10: rat internal control 2
10	ratSdha-qPCRR	TCAGAGCCTTTCACGGTGTC	
11	ratGpr55-qPCRF2	TCAGCCCGAGAAGGAACTGCTTC	11&12: rat Gpr55, flanking intron; isoform-specific; corresponding to 5&6 in mouse (used in Figure 7B)
12	ratGpr55-qPCRR2	TGGTCAGGTTGTCCACGAAAACGAA	

HPLC/MS

Extraction of LPIs from brain tissue

Prior to extraction, samples were moved from -80 °C storage to dry ice and weighed into 2.0 mL screw cap vials containing ~100 μL of disruption beads (Research Products International, Mount Prospect, IL). Each sample was normalized to 46 mg/mL using 100% methanol (Fisher Scientific) and homogenized for 10 cycles on a bead blaster homogenizer (Benchmark Scientific, Edison, NJ). Cycling consisted of a 30 sec homogenization time at 6 m/s followed by a 30 sec pause. In glass LC vials, 80 μL of Optima LC/MS grade water (Fisher Scientific, Waltham, MA) was combined with 80 μL of homogenate. Further extraction was performed by adding 160 μL of 100% chloroform and vortexing for 2 min. Entirety of sample was transferred to glass inserts and spun at 21,000 g for 3 min at 4 °C. For analysis, 20 μL of each sample was transferred to LC/MS vials containing glass inserts.

LC-MS/MS targeted LPI method

Standards of 16:0, 18:0 and 20:4 LPI (Avanti Polar Lipids) were prepared in ethanol at 1uM, 3uM, 10uM, 30uM, and 100uM and used to validate retention time and fragmentation pattern for each LPI. Samples were analyzed by UPLC-MS/MS with a targeted product reaction monitoring (PRM) method for 16:0, 18:0 and 20:4 LPI. The LC column was a Waters™ BEH-C18 (1.0 x 50 mm, 1.7 μm) coupled to a Dionex Ultimate 3000™ system and the column oven temperature was set to 25°C for the gradient elution. The flow rate of 0.1 mL/min was used with the following buffers; A) 60:40 acetonitrile:water, 10 mM ammonium formate, 0.1% formic acid and B) 90:10 isopropanol:acetonitrile, 10 mM ammonium formate, 0.1% formic acid. The gradient profile was as follows; 50-100%B (0-2.0 min), hold at 100% B (0.5 min), 100-50%B (2.5-3 min), hold at 50%B (3.0 min). Injection volume was set to 1 μL for all analyses (6 min total run time per injection). MS analyses were carried out by coupling the LC system to a Thermo Q Exactive HF™ mass spectrometer operating in heated electrospray ionization mode (HESI). Method duration was 6 min with a PRM scan in negative mode only. Global list for PRM contained $[M-H]^-$ theoretical masses for targeted LPIs. Spray voltage for was 3.5kV and capillary temperature was set to 320°C with a sheath gas rate of 25, aux gas of 10, and max spray current of 100 μA. Tandem MS scans utilized 30,000 resolution with a maximum IT of 100 ms, isolation window of 0.4 m/z, isolation offset of 0.1 m/z, and normalized collision energies (nCE) of 35. The minimum AGC target was 2e5 with an intensity threshold of 1e6. All data were acquired in profile mode. Duplicate standard curve points and samples were randomized for sequence injection. Standard curves were generated for each LPI. For quantitation, a background of 3x the average blank signal plus 10,000 counts was applied. Sample quantities were calculated using linear regressions to determine on column amount of each LPI. Assuming 100% extraction efficiency, calculated values were used to determine amount of LPI per mg of tissue.

QUANTIFICATION AND STATISTICAL ANALYSIS

Data analyses were performed using Clampfit (Molecular Devices, UK), Icy (http://icy.bioimageanalysis.org), and Prism 6 (GraphPad Software, USA) software. Data are presented as means ± SEM. For PTZ-induced seizure and mortality incidence, Chi-squared tests or Fisher's exact tests were used. For electrophysiological and molecular biological data, distributions passing Shapiro-Wilk test for normality were compared using a two-way student's t-test. Non-Gaussian distributions were compared using the non-parametric tests Wilcoxon signed rank test. For recordings pre- and post-drug application within a given cell, paired t-tests were used for comparisons. Events were normalized to the mean PSC frequency or amplitude during a 5 min window of baseline. For *in vitro* LPI experiments, intensities were normalized to the average of the vehicle-treated condition. For 3 or more independent comparisons (including electrophysiological recordings, HPLC, qPCR, ICC, and immunoblots), a one-way ANOVA followed by post-hoc testing (e.g. Dunnett's or Bonferroni's) was performed. Differences were considered significant at $p \leq 0.05$.